Journal of Contaminant Hydrology 216 (2018) 10–26

Contents lists available at ScienceDirect

Journal of Contaminant Hydrology

journal homepage: www.elsevier.com/locate/jconhyd

Numerical prediction of the long-term evolution of acid mine drainage at a waste rock pile site remediated with an HDPE-lined cover system

Murugan Ramasamy, Christopher Power*, Martin Mkandawire

Verschuren Centre for Sustainability in Energy and the Environment, Cape Breton University, Sydney, Nova Scotia, Canada

ARTICLE INFO

Keywords:
Contaminant remediation
Cover system
High-density polyethylene (HDPE)
Numerical simulation
FEFLOW
Sulfate concentration

ABSTRACT

Remediation at former mining sites containing waste rock piles (WRPs) commonly involves the installation of a cover system over the waste rock to limit water and oxygen ingress and attenuate the impacts of acid mine drainage (AMD) to the environment. Cover systems containing high-density polyethylene (HDPE) liners have the attributes to be highly effective; however, their performance over the long-term is unknown. The objective of this study was to assess the long-term effectiveness of an 'in-service' HDPE-lined cover system for reducing AMD contamination at WRP sites. A numerical investigation of a former mining site containing a large WRP reclaimed with an HDPE cover is presented. A 3-D groundwater flow and contaminant transport model of the site was developed in FEFLOW to predict the spatial and temporal evolution of AMD over 100 years. Field parameters observed at 46 monitoring wells over a 5-year monitoring period (including hydraulic head, recharge, hydraulic conductivity and water quality) were used as key input and calibration parameters. The HDPE cover significantly reduced both water recharge to the waste rock (i.e., 512 to 50 mm/year) and AMD seepage to groundwater. Both the groundwater flow and contaminant transport (sulfate was used as an AMD tracer) components of the model were calibrated and verified to the observed field data, with strong correlations evident between observed and simulated hydraulic heads and sulfate concentrations, respectively. Long-term model predictions of AMD evolution indicated significant and continual reductions in sulfate concentrations over time at all well locations. Background concentration levels (25 mg/L) are expected to be reached within 40 years. This study has demonstrated that HDPE-lined cover systems can be highly effective in reducing AMD loading from WRPs and its impacts on the receiving environment.

1. Introduction

Environmental impacts associated with active and abandoned coal mine sites worldwide are well-documented. Mining activities worldwide have left a legacy of contaminated sites that contain waste rock piles (WRPs). WRPs are large anthropogenic created landforms that typically range in height from 10 m to 30 m and can have surface areas up to several km^2 (Blowes, 1997). Most WRPs contain sulfidic minerals such as pyrite and pyrrhotite, which when exposed to atmospheric conditions (oxygen and water) can initiate and sustain a process commonly referred to as acid mine drainage (AMD). AMD produces an acidic sulfate-rich leachate that can then further dissolve other minerals in the host rock and become enriched with iron and other toxic metals (INAP, 2014; Nordstrom et al., 2015). The formation of AMD and its seepage into surrounding groundwater and surface watercourses can occur for extended periods (i.e., centuries or even millenia), resulting in a long-term source of environmental contamination (e.g., Simate and Ndlovu, 2014; Amos et al., 2015).

Cover systems are commonly installed over the WRP to limit the influx of atmospheric oxygen and meteoric water to the reactive waste material, thereby preventing and/or controlling AMD formation (e.g., Kefeni et al., 2017; Power et al., 2018a). Cover systems can be simple or complex, ranging from a single layer of earthen material to multiple individual layers of different material types, including native soils, oxygen-consuming organic materials and geosynthetic materials (MEND, 2004; Power et al., 2017). The design of a cover system is, in most cases, site-specific and depends on the climatic conditions prevailing at a given site.

Single layer covers act to minimize water influx by maximizing near-surface storage of moisture with subsequent release by evapotranspiration (e.g., Power et al., 2018a, 2018b). As a result, they are most effective in arid or semi-arid regions where potential evaporation exceeds precipitation (Scanlon et al., 2005; O'Kane and Ayres, 2012). Multi-layer covers utilize the capillary barrier concept to maintain a

* Corresponding author.
E-mail addresses: murugan_ramasamy@cbu.ca (M. Ramasamy), chris_power@cbu.ca (C. Power), martin_mkandawire@cbu.ca (M. Mkandawire).

https://doi.org/10.1016/j.jconhyd.2018.07.007
Received 15 December 2017; Received in revised form 8 June 2018; Accepted 22 July 2018
Available online 24 July 2018
0169-7722/

high degree of saturation (at least 85%) in one or more of its layers (e.g., Yanful et al., 1999). This high saturation layer increases moisture storage for subsequent release by runoff and/or evapotranspiration (e.g., Hopp et al., 2011) and provides an effective oxygen barrier due to the low diffusivity of oxygen in water (Yanful, 1993). While multi-layer covers have been used in all climatic regions, they have been unable to maintain a high degree of saturation throughout the year. The use of enhanced soil layers such as compacted clay liners has resulted in improved water retention capacities (e.g., Benson et al., 1999) but they are strongly affected by desiccation and freeze-thaw cycling (e.g., Othman and Benson, 1993; Albrecht and Benson, 2001).

Geosynthetic materials are being increasingly used in one or more of the layers in multi-layered WRP cover systems to increase performance with reduced water infiltration and oxygen influx (MEND, 2012). Geosynthetic clay liners (GCLs), consisting of bentonite clay supported by geotextiles, have been widely used (e.g., Cazaux and Didier, 2000). While they have performed well as a moisture barrier (e.g., Benson et al., 2007), their effectiveness as an oxygen-diffusion barrier remains questionable due to their short diffusion path length and susceptibility to desiccation (e.g., Meer and Benson, 2007). Geomembranes used in mining or landfill-related applications are usually high density polyethylene (HDPE), which provides a highly effective barrier to water and oxygen (e.g., Rowe, 2005).

While pristine HDPE liners exhibit excellent attributes, in situ performance can be affected by various elements in both the short and long term. In the short term, on-site HDPE installation has a significant impact on the development of wrinkles, defects and deformations (e.g., Giroud et al., 1992; Rowe, 2012). Chappel et al. (2012) demonstrated that wrinkles develop rapidly in HDPE exposed to solar heating, suggesting that an overlying layer should only be placed over the HDPE at certain times/temperatures (Rowe et al., 2012). All installed HDPE liners have some level of defects due to improper seaming or puncturing during placement of overlying material. Numerous methods have been established for estimating leakage rates through wrinkles and defects (e.g. Giroud et al., 1992; Rowe, 2012).

Site-specific environmental elements, including service temperature, strongly influence long-term HDPE ageing and performance. The service life of covered (unexposed) HDPE was shown to be 450, 265 and 70 years at 20, 25 and 40 °C, respectively, indicating that higher temperatures results in shorter service life (Sangam and Rowe, 2002; Koerner et al., 2011; Rowe and Ewais, 2015). Furthermore, covered HDPE maintains performance for significantly longer than exposed HDPE. Rowe et al. (2009) demonstrated that HDPE can maintain performance levels when exposed to leachates and high temperature extremes. Sangam and Rowe (2002) indicated that the service life would be even greater when only exposed to unsaturated soil. Based on the aforementioned studies, HDPE liners can provide an effective, long-term barrier in WRP cover systems containing an overlying soil layer and in climates where service temperatures are typically < 30 °C.

Despite this potential, HDPE liners are primarily used at mining sites for liquid containment and basal liners (e.g., Benson, 2000; Lupo and Morrison, 2007), with few HDPE-lined cover systems installed at WRPs. The majority of studies assessing the performance of these cover systems have been limited to small-scale test cover plots (e.g., Ayres et al., 2003; Adu-Wusu and Yanful, 2006), with only a handful performed at full-scale 'in-service' WRPs (e.g., Meiers et al., 2011; Power et al., 2017). Meiers et al. (2011) monitored oxygen concentrations and water infiltration rates for one year and demonstrated limited atmospheric flux into the waste rock. Power et al. (2017) monitored a range of parameters, including oxygen/water influx and water quality in environmental receptors, across a WRP site reclaimed with an HDPE-lined cover system. Significant reductions in oxygen/water influx and improvements in water quality highlighted the effectiveness of cover performance. While these field studies have been able to directly indicate HDPE cover performance, they are limited to the short-term (≤ 5 years). No information is available on long-term HDPE cover performance and associated AMD evolution.

Numerical models are widely used to predict the long-term evolution of groundwater contaminants during and/or following remediation, including chlorinated solvents (e.g., Power et al., 2014) and landfill leachate (e.g., Sizirici and Tansel, 2010). Numerical models in WRP studies have been used to examine various processes occurring within the waste rock, ranging from unsaturated water flow in hypothetical WRPs (e.g., Fala et al., 2005) to complete representations of sulfide oxidation (including heat transport, diffusive and convective air transport, spatially and temporally dependent pyrite oxidation rates) at full-scale WRPs (e.g., Lefebvre et al., 2001; Molson et al., 2005; Fala et al., 2013). Numerical studies have also been performed to simulate and assess the effects of WRP covers on oxygen and water influx to the waste rock (e.g., Kim and Benson, 2004; Song and Yanful, 2008).

While complex hydrological and geochemical processes within WRPs have been simulated, few, if any, studies have assessed the spatial and temporal evolution of AMD at WRP sites (including WRP and receiving environment) following remediation. Although not used for WRP investigations, numerical models have been used to simulate other contaminants in groundwater in analogous studies. For example, Bordeleau et al. (2008) modeled dissolved RDX and nitrate at an air weapons range site in Alberta, Canada to predict whether the contaminants pose a threat to nearby surface water receptors, while Şengör and Ünlü (2013) examined the extent of acrylonitrile plume migration at an industrial spill site in Turkey.

In this study, a numerical investigation is presented of a remediated mining site that includes a large WRP overlain with an HDPE-lined cover system. A three-dimensional (3-D) transient groundwater flow and contaminant transport model of the study site was developed in FEFLOW and then calibrated and verified with hydrogeological and geochemical data collected during five years of post-remediation monitoring. The model was then simulated for 100 years to predict the spatial and temporal evolution of AMD and illustrate the long-term effectiveness of HDPE cover systems installed at WRPs.

2. Study site

2.1. Site description

2.1.1. Waste rock pile

The Sydney Coalfield in Nova Scotia, Canada is the oldest coal field in North America, with underground mining occurring from the early 1700s to the early 2000s. These historic mining operations included > 50 underground mines that produced over 500 million tonnes of coal (Power et al., 2018a). In 2001, Enterprise Cape Breton Corporation (ECBC) commenced a mine site closure program throughout the coal field which was managed by Public Works and Government Services Canada (PWGSC, 2013). A number of WRP sites were remediated as part of this program, including the Scotchtown Summit WRP located in Scotchtown, approximately 15 km north of Sydney. Fig. 1 presents a plan view of the WRP and surrounding area which is referred to as the Scotchtown Summit Study Area (SSSA). The perimeter of the SSSA, which has an area of 12 km^2, is indicated by the black dashed lines.

The SSSA was used as a dump for the placement of waste rock from nearby mine collieries between 1911 and 1973. The waste rock was reprocessed from 1981 to 1987 to recover coal, with this process expanding the WRP footprint to 44 ha. Extensive remediation that commenced in 2009 included reshaping and consolidation of the pile, which reduced the footprint to 37 ha, and the installation of a cover system. The WRP contains approximately 1.5 million m^3 of waste rock fill, with slopes on the pile ranging between 1% and 10% on top, and between 4% and 20% on the sides. Detailed surface topography was determined from light detection and ranging (LiDAR) with elevations in the SSSA ranging from 6 masl to 59 masl.

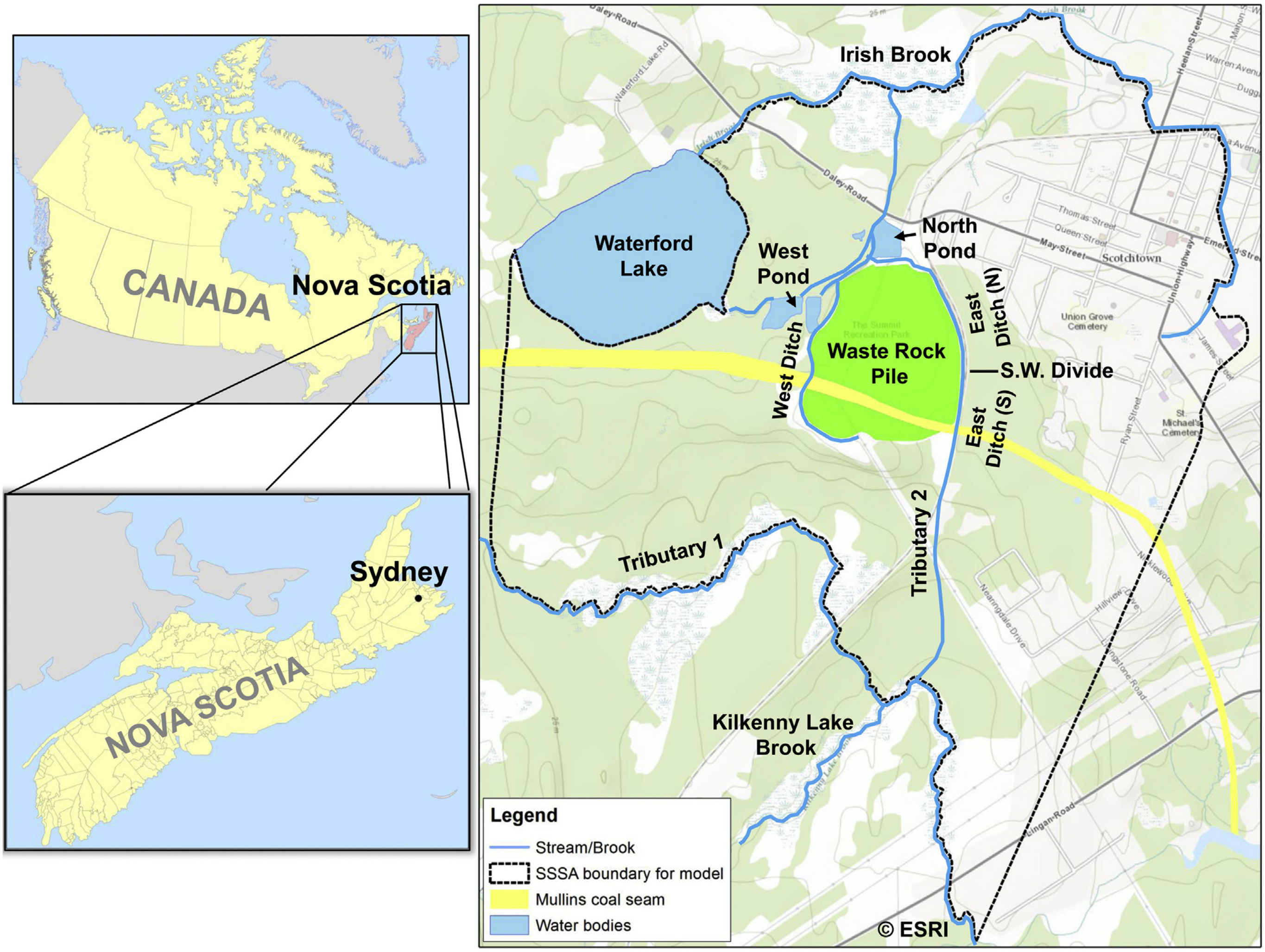

Fig. 1. The location of the Summit WRP site in Scotchtown, Nova Scotia, Canada. The site map indicates the location of the WRP, groundwater monitoring wells and surface water bodies and features.

2.1.2. Climate

The study area experiences a humid continental climate, experiencing large seasonal temperature variations, with warm to hot summers and cold to severely cold winters. Based on long-term data recorded at the nearby Sydney Airport, mean annual precipitation (PPT) and potential evaporation (PE) are approximately 1500 mm and 650 mm, respectively (Environment Canada, 2017).

2.1.3. Geology

Prior to remediation, various investigations were performed to characterize geology, hydrogeology and geochemistry. A number of geologic units exist within the SSSA which are listed in Table 1. Overburden material comprises waste rock, peat and till. The waste rock is characterized by grey, silty clayey sand with gravel, and ranges in thickness from approximately 1.4 m to 10 m, with the thickest deposits at the center of the WRP. It consists of iron-stained shales, sandstone and siltstone, mixed with coal fines. The WRP is underlain by a brown, silty sandy till ranging in thickness from 2 m to 4 m. In some areas, the waste rock and till units are separated by an organic peat layer that represents the original ground surface prior to placement of the WRP.

The till is underlain by bedrock which constitutes the Lower Morien Group comprising massive fine- to medium-grained sandstone, with some interbedded mudstone, conglomerate and thin coal seams. Bedrock strikes essentially from east-to-west and dips to the north at 30 to 40°. A 1.5 m thick coal seam, referred to as the Mullins Coal Seam, strikes roughly east-to-west beneath the southern portion of the WRP.

Table 1
Summary of geologic units in the study area.

Geologic unit	Hydraulic conductivity (m/s)	Thickness (m)	Model layer
Cover material[a]	1.2×10^{-7}–2.8×10^{-6}	0.5	1
Waste rock[a]	1.0×10^{-6}	1–10	2 to 4
Organic material[a]	–	0.5	5
Till[b]	1.0×10^{-7}–6.5×10^{-6}	2–4	6
Shallow bedrock	7.0×10^{-6}–4.1×10^{-5}	10	7 to 8
Intermediate bedrock	1.0×10^{-5}–1.6×10^{-5}	20	9 to 12
Deep bedrock	5.0×10^{-6}–1.9×10^{-5}	60	13 to 18
Mullins Coal Seam[c]	2.0×10^{-5}–4.0×10^{-6}	10–60	7 to 18

[a] Referred to as overburden material inside the pile footprint.
[b] Referred to as overburden material outside the pile footprint.
[c] Mullins Coal Seam is only a small portion of each bedrock unit and corresponding model layer.

Hydraulic conductivity values used in each geologic unit were obtained from geological investigations completed before and during remedial activities. Although geological logs for each unit were distributed across the SSSA, the range of measured hydraulic conductivities for each unit are within one to two orders of magnitude, as shown in Table 1.

2.1.4. Hydrogeology

The SSSA straddles a drainage divide between the Irish Brook watershed to the north and Kilkenny Lake Brook watershed to the south. This divide is indicated in Fig. 1. The west, north and east(north) perimeter ditches of the WRP drain north into an alkaline treatment pond (North Pond) and subsequently northwards into Irish Brook. The east(south) perimeter ditch flows southwards to Tributary 1 and Tributary 2 before ultimately draining into Kilkenny Lake Brook. In terms of groundwater, it has historically flown from the topographical high to the northeast of the WRP towards the WRP. As it flows through the WRP, it is deflected by a groundwater divide existing in the south of the WRP that is influenced by the presence of the Mullins Coal Seam. As a result, groundwater flows predominantly from the WRP downgradient towards the west, northwest and south.

2.1.5. AMD contamination

Extensive AMD contamination was confirmed at the SSSA prior to remediation. Geochemical analysis of groundwater collected from monitoring wells distributed across the SSSA indicated AMD-impacted groundwater characterized by low pH and elevated concentrations of sulfate and dissolved metals. As expected, the AMD contaminant plume coincides with the dominant groundwater flow directions, with highest AMD impacts observed within the pile footprint and in downgradient regions to the west, northwest and south. Similarly, surface water collected from the various water bodies in the SSSA also confirmed the impacts of AMD.

2.2. Site remediation and field monitoring

The key site remedial objectives were the (i) protection of water quality in Waterford Lake, (ii) protection of Tributary 1 and Tributary 2 to Kilkenny Lake Brook with respect to fish habitat, and (iii) improvement in the quality of surface water in Irish Brook.

2.2.1. Cover system

A 0.15 m thick bedding sand layer was first placed over the exposed waste rock and then overlain with a 1.5 mm (60 mil) thick HDPE geomembrane, which is the most commonly used geomembrane at mine sites (Thiel and Smith, 2004). A protective layer of geotextile fabric was placed on top of the HDPE, which in turn was overlain with a 0.5 m thick layer of imported till material. The 0.5 m thickness was used to allow sufficient space for typical vegetation rooting above the HDPE liner. This soil layer was then hydroseeded to promote vegetation growth and provide a geomorphically stable landform.

This cover type was installed to significantly reduce oxygen and water flux into the waste rock and eliminate contaminated surface water runoff from the previously exposed waste rock. The limited AMD generation and release would consequently improve groundwater and surface water quality and ensure remedial objectives are achieved.

2.2.2. Hydrogeochemical monitoring

A comprehensive field monitoring program was performed at the SSSA between 2012 and 2016. Various instrumentation was installed to monitor key parameters in the atmosphere, cover system, waste rock, groundwater and surface water. Fig. 2 indicates the location of the field instrumentation. A meteorological station automatically measures rainfall, air temperature, relative humidity, wind speed and direction, barometric pressure, and snowdepth. An interflow collection system quantifies lateral flow throughout the cover, while a weir measures surface runoff flows from the WRP. Four soil monitoring stations (SMS) were located across the WRP to continuously monitor soil moisture, suction and temperature at 9 depths within the cover and shallow waste rock (ranging from 0.05 m to 2.37 m). Pore-gas sampling ports were also installed at 3 depths (0.40 m to 0.90 m).

Four continuous multi-channel tubing (CMT) wells were installed through the waste rock and into the underlying shallow bedrock. The CMT wells monitored soil temperature and differential pressure at larger depths within the waste rock (1.9 m to 9.5 m), while also permitting pore-gas sampling. Groundwater levels could be collected from the base of each CMT well along with water samples for geochemical analysis. Aside from pore-gas and groundwater levels/samples, all aforementioned parameters were automatically monitored every hour between January 2012 and December 2016. Manual collection of pore-gas concentrations at each SMS and CMT well, and groundwater levels and geochemical analysis at each CMT well, was conducted almost monthly between June 2012 and November 2016 (see Table 2). A full description of the field instrumentation and analysis of the measured parameters is presented by Power et al. (2017).

A total of 42 monitoring wells are screened within the various geologic units within the SSSA. As shown in Fig. 1, 3 wells are located upgradient to the northeast of the WRP, 14 wells are located within the pile footprint, and the remaining 25 wells are located in downgradient locations. Table 2 summarizes the sampling events for groundwater levels and geochemistry at the 42 monitoring wells. The wells were sampled each Spring, Summer and Fall between August 2014 and July 2016 to monitor AMD evolution following remediation. AMD conditions prior to the completion of remediation are available from sampling performed between February 2009 and November 2011.

Surface water sampling was also conducted at various locations along each watercourse in the SSSA, including the WRP perimeter ditches, Irish Brook, Waterford Lake, Tributary 1 and Tributary 2.

2.2.3. Landform stability and vegetation

Vegetation surveys, erosion surveys and aerial inspections were conducted annually to monitor the stability of the landform and evolution of the vegetation cover. Vegetation and changes in species composition on the WRP significantly influence the geomorphic stability and control erosion, soil texture and water holding capacity. Furthermore, root depth and densities need to be inspected to assess the risk of excessive root growth and penetration of the HDPE geomembrane.

2.3. Key field parameters

The following subset of field parameters was required to develop, calibrate and verify the transient flow and contaminant transport model:

(i) Hydraulic conductivity

Hydraulic conductivity values are available for each geologic unit in the SSSA, as shown in Table 1. As evident, the range of hydraulic conductivities for each unit is quite narrow and each unit is assumed to be homogeneous. Anisotropy is implemented using different values for horizontal and vertical hydraulic conductivity. A horizontal:vertical ratio (K_h/K_v) of 10 is typically used in groundwater studies (e.g., Elango et al., 2012; Anderson et al., 2015) and was assigned to the initial model domain.

(ii) Hydraulic head

The groundwater levels measured throughout the 5-year monitoring period are hereafter referred to as the observed hydraulic heads in the model.

(iii) Groundwater recharge

Groundwater recharge is based on land use and/or land cover. Three regions of differing land cover and recharge rates exist in the SSSA: forested, urbanized and WRP, as highlighted in Fig. 2. The

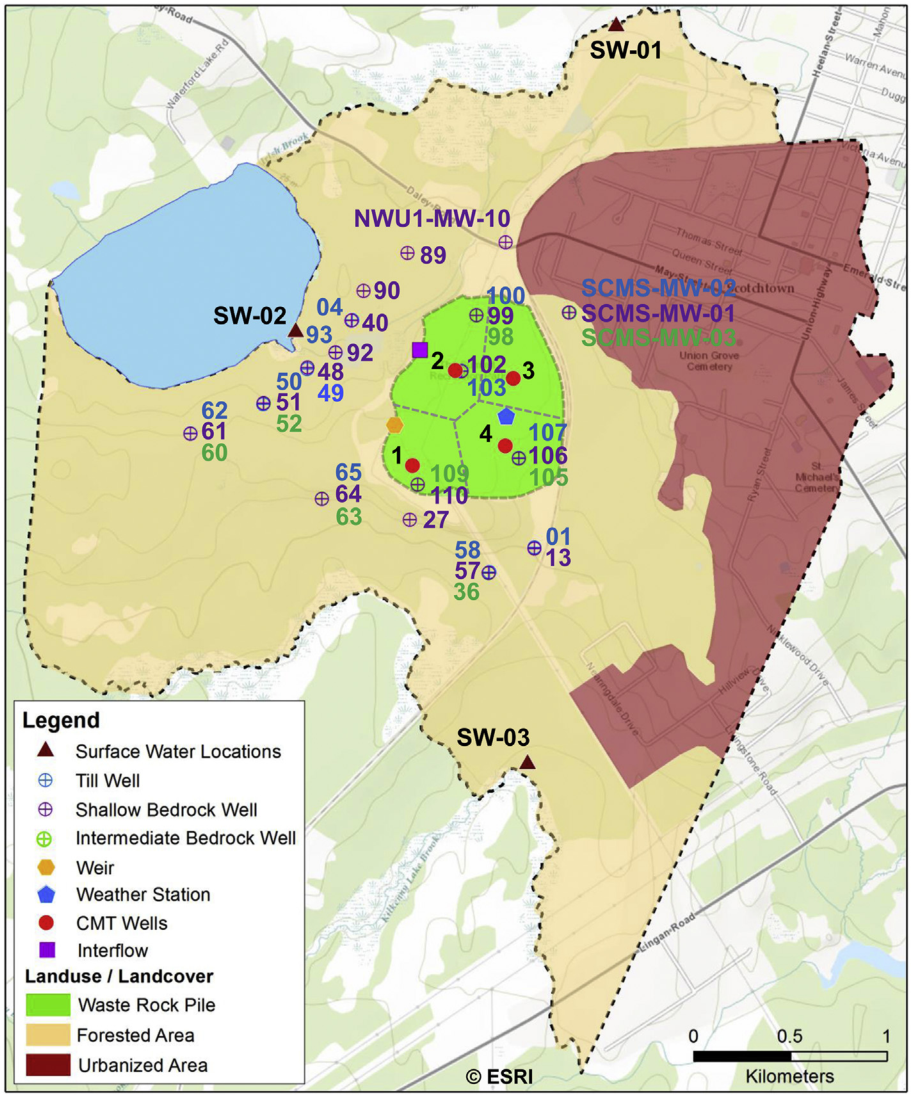

Fig. 2. Site map of the study area indicating the location of field instrumentation. The differing land use regions for forest, urban and WRP are highlighted by the brown, purple and green regions, respectively. The source 'polygons' associated with each CMT well are indicated by the dashed lines within the WRP footprint. (For interpretation of the references to colour in this figure legend, the reader is referred to the web version of this article.)

Table 2
Summary of groundwater sampling (levels and geochemistry) in the study area.

Instrument	Number	Geologic Unit	Pre-Cover[a]	Post-Cover[b]
CMT Wells	4	Shallow bedrock	–	Jun 2012–Dec 2016 (30)
Monitoring Wells	42	Waste rock, till, shallow bedrock, interm. bedrock	Feb 2009–Nov 2011 (12)	Aug 2014–Jul 2016 (9)

[a] The CMT wells were only installed in 2011 so 'pre-cover' groundwater information does not exist.

[b] The number of samples collected in the stated sampling period is given in parentheses.

recharge rates in forested and urbanized areas are established from previous studies in the Sydney Coalfield (e.g., King et al., 2003). Based on various factors such as geology, surface cover, topography, rainfall and snowfall, recharge rates of 325 mm/year and 175 mm/year are assigned to the forested and urbanized regions, respectively.

The recharge rate assigned to the WRP area is the net percolation (NP) through the HDPE-lined cover into the waste rock. The primary mechanism for NP to occur is leakage through defects that inevitably develop due to accidental punctures and improper seaming during installation (e.g., Rowe, 2012). As a result, the number and sizes of defects in the liner directly influence the leakage rate (Needham et al., 2006). Numerous studies at various landfills have demonstrated the mean defect density in HDPE liners ranges from 12.9 holes per hectare (holes/ha) to 34.4 holes/ha (e.g., Rollin et al., 2002; Nosko and Touze-Foltz, 2000; Needham et al., 2004). Colucci and Lavagnolo (1995) demonstrated that 50% of geomembrane holes had an area of $< 100\ \mathrm{mm}^2$ (equivalent radius < 5.64 mm).

Numerous empirical and analytical equations have been established to estimate leakage rates through holes (e.g., Giroud et al., 1992; Touze-Foltz and Giroud, 2003; Cartaud et al., 2005) or defects coincident with, or adjacent to, wrinkles (e.g., Rowe et al., 2012). For the study site, it is assumed that the geomembrane was installed during adequate (cooler) temperatures to minimize wrinkle development (e.g., Take et al., 2007), with only holes/tears occuring. Touze-Foltz and Giroud (2003) established the following solution for determining the leakage rate through circular defects with diameters ranging from 2 mm to 20 mm:

$$Q = C_a \cdot a^{0.1} \cdot k_s^{0.74} \cdot h_w^{0.9}\,[1 + 0.1(h_w/H_s)^{0.95}] \tag{1}$$

where Q is the leakage rate [m^3/s], C_a is the contact quality factor (0.21 for good and 1.15 for poor) [−], a is the area of the defect [m^2], k_s is the saturated hydraulic conductivity of the underlying material [m/s], h_w is the head of water above the liner [m], and H_s is the thickness of the underlying material [m]. Eq. (1) is widely used to estimate leakage rates through defective geomembranes (e.g., Li et al., 2012; Agbenyeku et al., 2017) and is used to estimate recharge to the WRP in this study. The head of water was determined by pore-water pressure sensors at the SMSs. The k_s and H_s for the bedding sand are 1×10^{-7} m/s and 0.15 m, respectively. Poor contact was assumed between the HDPE liner and the underlying bedding sand. It was assumed that 20 holes/ha exist with an area of 79 mm^2 (radius = 5 mm), which lies within the typical ranges reported in previous studies (e.g., Colucci and Lavagnolo, 1995; Needham et al., 2004; Meiers and Bradley, 2017).

Annual water balances were developed to evaluate water dynamics in the cover system and were comprised of the following components (e.g. Meiers et al., 2009):

$$PPT = R + AET + \Delta S + LP + NP \tag{2}$$

where ΔS is change in water storage within the cover material [mm]. NP was calculated as the residual of Eq. (2), with these water balance NP rates similar to, and thereby validating, the NP rates estimated in Eq. (1). A full description of the annual water balances developed for the site between 2012 and 2016 is provided in Power et al. (2017).

Table 3 presents the annual recharge rates for the differing land use regions in the study area. In addition to the recharge rate for the covered WRP, the rate that would exist with no cover is also presented. This 'pre-cover' rate is based on the NP/PPT ratio of 34% demonstrated on similar waste rock/fill material by King et al. (2003). Table 3 highlights the significant reduction in WRP recharge due to the cover system with a reduction in NP from 34% to 3% of PPT. Monthly varying groundwater recharge was assigned to each recharge zone (Fig. 2) of the transient model as a percentage of PPT.

The recharge and PPT measured each month throughout the 5-year monitoring period are used to develop a monthly recharge rate as a percentage of PPT. To obtain long-term predictions of recharge while accounting for climate change patterns, a climate period of 30 or more years is used. In this study, the monthly recharge (% PPT) is integrated with the monthly climate data recorded between January 1981 and December 2010 (Canadian Climate Normals) to provide long-term recharge for the predictive model.

(iv) AMD contaminant source

The geochemical source term for the WRP is taken from representative wells installed within the pile footprint. The 4 monitoring wells screened in the waste rock – SSSA-MW-101, SSSA-MW-104, SSSA-MW-108 and SSSA-MW-112 – would normally provide the most representative water quality seeping from the WRP; however, each of the 4 wells were dry during all sampling events and wells screened below the waste rock are instead used. Of these 14 wells, the sampling density at the 4 CMT wells (30 samples) is much higher than at the 10 monitoring wells (9 samples) between June 2012 and December 2016, and would provide improved calibration and verification. As a result, the geochemical data at the 4 CMT wells is used to represent the AMD source.

Sulfate is commonly used as a key AMD indicator or geochemical tracer due to its high persistence in groundwater relative to other AMD indicators such as iron and aluminum. Sulfate concentrations at the 4 CMT wells are used to represent the AMD source in the WRP, while sulfate concentrations at all 42 monitoring wells are used to represent the AMD groundwater plume distributed across the SSSA.

Table 3
Groundwater recharge values (mm/year) assigned to different land cover regions.

Region	2012	2013	2014	2015	2016
WRP recharge (no cover)[a]	442	512	549	521	570
WRP recharge (with cover)	41	43	54	54	79
Forested recharge	325	325	325	325	325
Urbanized recharge	175	175	175	175	175

[a] Estimated as 34% of precipitation (King et al., 2003).

3. Model development

A 3-D transient groundwater flow and contaminant transport numerical model was developed using FEFLOW 6.2 to analyze and predict long-term groundwater flow and AMD contaminant at the study site. FEFLOW is a 2-D and 3-D finite element modeling package that can simulate steady or transient state, fluid density, coupled flow and mass transport (Diersch, 2014). It is widely used in hydrogeological studies (e.g., Bordeleau et al., 2008; Elango et al., 2012; Chopra et al., 2013).

3.1. Model discretization

The full SSSA area of 12 km^2 was discretized into a 3-D finite element mesh, consisting of 297,108 triangular finite element cells. The modeled domain integrates both the saturated zone, corresponding to the till and underlying bedrock aquifers, and the unsaturated zone, corresponding to the upper part of the till and the WRP. Mesh discretization was optimized based on site information with finer discretization employed near the WRP and water bodies. Fig. 3a presents the 3-D model domain, while Fig. 3b and c present 2-D vertical cross-sections.

The model domain was subdivided vertically into 18 layers with variable thickness to represent the various geologic units. The top 5 layers represent the overburden within the pile footprint which comprises cover material, waste rock and organic material/peat. Layer 6 represents the till unit that both underlies the WRP and is the overburden outside the pile footprint. The next 12 layers are used to represent the shallow, intermediate and deep bedrock units. Table 1 lists each geologic unit and associated model layer.

3.2. Boundary and initial conditions

The modeled area is based on the extent of the SSSA which is delineated on all sides by specific hydrogeological and physical boundaries. Fig. 3a indicates the boundary conditions used. As the southwestern and eastern boundaries are watershed boundaries, they are both considered as a no-flow boundary. The western boundary is also considered as a no-flow boundary. The northern boundary corresponds with Irish Brook. As the streambed elevation of Irish Brook is assumed to coincide with the till/shallow bedrock interface, layers 6 and 7 in the northern boundary are considered as specified head boundary with all remaining layers considered as a no-flow boundary. The southern boundary corresponds with Tributary 1 and is considered as a specified head boundary in all layers. Similarly, the boundary along Waterford Lake is considered as a specified head boundary which corresponds to the measured surface water level in the lake (i.e., 25.5 masl).

The base of the model domain, where it is assumed that groundwater flow is near-horizontal and water does not leave or enter, is considered as a no-flow boundary. A river head boundary condition was applied to all surface water bodies inside the study area, including ponds and drainage ditches. The top boundary condition, representing the land surface exposed to the atmosphere, is expressed as a transient flux equal to seasonal variations of groundwater recharge.

The initial hydraulic head distribution for the model was based on groundwater elevations from the 'starting point' of the 4 CMT wells (June 2012) and 42 monitoring wells (mean February 2009 to November 2011).

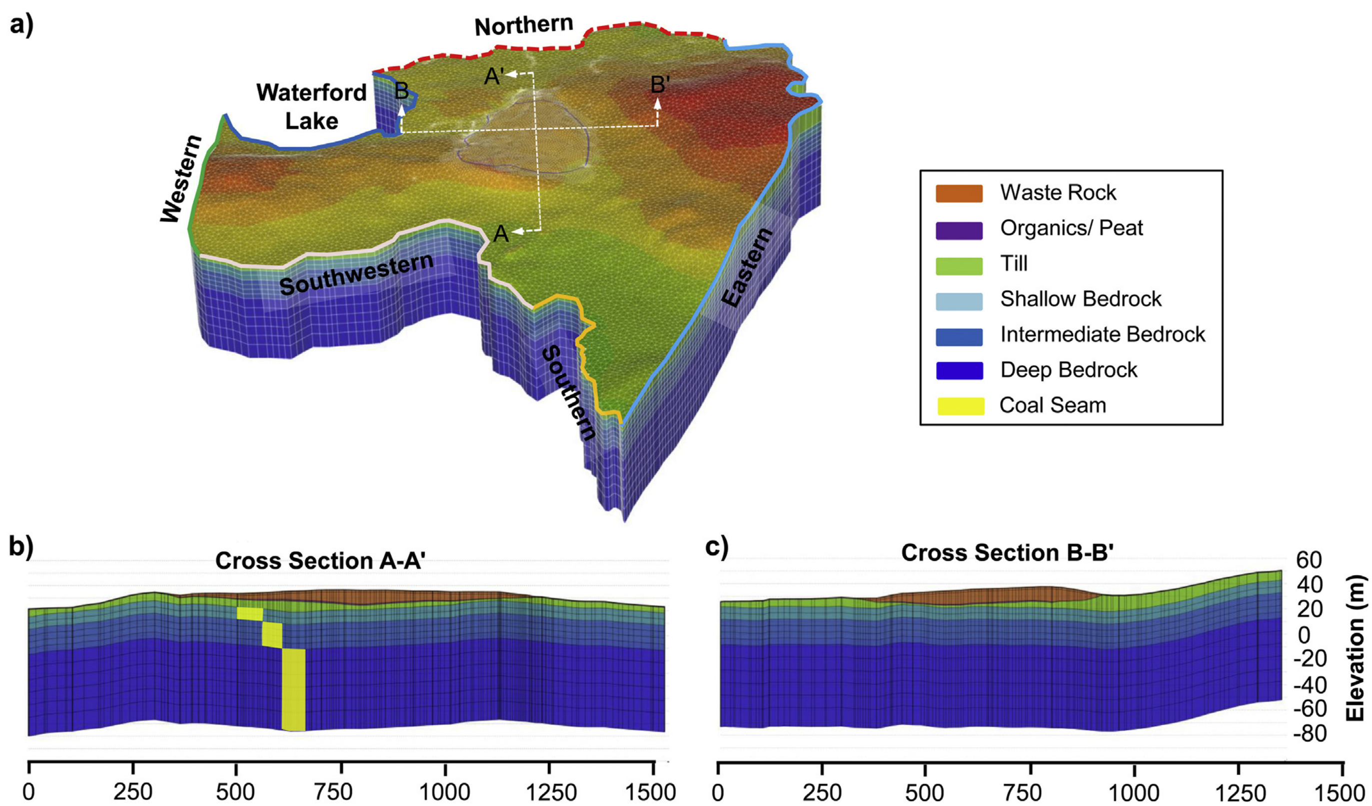

Fig. 3. (a) discretized 3-D model domain of the study area and associated vertical cross-sections (b) A-A' and (c) B-B′. The different boundary conditions are identified in (a). Variations in surface topography are visible by the contouring in (a) with highest elevations in red and lowest elevations in green.

3.3. Groundwater flow model

3.3.1. Model calibration

The groundwater flow model was first calibrated in steady state conditions to achieve the best correlation between the simulated hydraulic heads and the observed hydraulic heads in each of the till, shallow bedrock and intermediate bedrock units. The primary variables that were adjusted within an allowable range for the trial-and-error calibration were boundary condition, hydraulic conductivity and groundwater recharge. For example, the western boundary was initially assumed as a no-flow boundary but was altered to a specified head boundary during model calibration. The calibration was performed until the mean error of simulated versus observed heads was minimized as much as possible in all units. In Fig. 4, a summary of the calibration is presented in the form of a scatter plot diagram of 46 simulated heads versus observed heads. It is evident that the simulated heads correlate well with the observed heads with a root mean squared (RMS) error of 2.1 m. This is well within the acceptable range and is similar to other studies (e.g., 2.9 m in Orban et al., 2010).

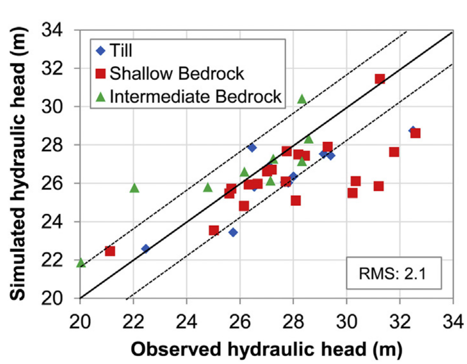

Fig. 4. Steady state comparison of simulated and observed hydraulic heads in each geologic unit. The solid black line represents the 1:1 and the dashed lines represents one standard deviation of ± 1.9 m.

3.3.2. Model verification

The calibrated steady state model was then verified against the time-varying hydraulic heads. The calibrated steady state conditions, including hydraulic heads and hydraulic conductivity, were used as initial conditions for the transient flow model. The transient model was simulated for the time period between June 2012 and December 2016 which coincides with the field monitoring period and the availability of observed hydraulic heads (see Table 2). Since a significant amount of the hydraulic heads at the CMT wells were measured monthly, a 30-day time step was used. While the transient model was mainly used for verification, some minor trial-and-error adjustments (calibration) were made to fine-tune some of the time-varying input parameters such as variable head boundary and groundwater recharge. Table 4 presents the initial and calibrated horizontal and vertical hydraulic conductivities used in the model.

A comparative analysis between the temporal variation in simulated and observed hydraulic heads indicated a strong correlation. Fig. 5 presents the simulated and observed heads versus time at selected wells in each geologic unit at key groundwater flow regions in the study area: beneath the WRP, downgradient (west) of the WRP and downgradient (south) of the WRP. It is evident that the simulated heads correlate well with the observed heads in each region and unit over the 5-year time period. For instance, seasonal variations in observed heads are repeated in the simulated heads at all wells. The CMT wells re a good indicator of correlation quality due to their high sampling density. Larger discrepancies are evident at some wells, which can be expected since the calibrated steady state model assumed homogeneity in each geologic unit and does not account for local variations in geological conditions.

Fig. 6 presents a scatter plot diagram of simulated versus observed

Table 4
Initial and calibrated hydraulic conductivity values used in the model.

Geologic unit	Initial		Calibrated	
	Horizontal hydraulic	Vertical hydraulic	Horizontal hydraulic	Vertical hydraulic
	cond. (m/s)	cond. (m/s)	cond. (m/s)	cond. (m/s)
Cover material	4.6×10^{-7}	4.6×10^{-8}	4.6×10^{-7}	4.6×10^{-8}
Waste rock	1.0×10^{-6}	1.0×10^{-7}	1.0×10^{-6}	1.0×10^{-7}
Till	6.5×10^{-6}	6.5×10^{-7}	6.5×10^{-6}	6.5×10^{-8}
Organic material/ peat	1.0×10^{-7}	1.0×10^{-7}	1.0×10^{-7}	1.0×10^{-7}
Shallow bedrock	4.1×10^{-6}	4.1×10^{-7}	3.0×10^{-5}	3.0×10^{-7}
Intermediate bedrock	1.6×10^{-5}	1.6×10^{-6}	1.5×10^{-5}	1.5×10^{-7}
Deep bedrock	1.9×10^{-5}	1.9×10^{-6}	5.0×10^{-6}	5.0×10^{-8}
Mullins Coal Seam	1.6×10^{-7}	1.6×10^{-7}	1.0×10^{-8}	1.0×10^{-8}

hydraulic heads at all 46 CMT and monitoring wells over time. Good agreement is evident between the simulated and observed heads at all locations and units. The RMS error was 2 m. It is evident that the transient flow model has been well calibrated and verified to observed head values over the 5-year monitoring period.

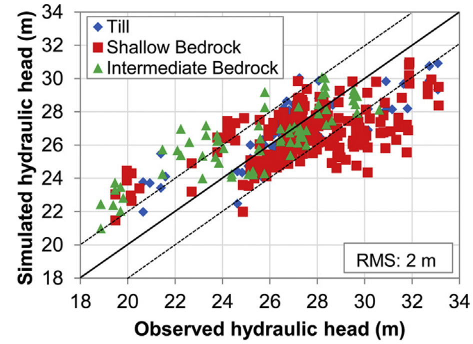

Fig. 6. Transient state comparison of simulated and observed hydraulic heads in each geologic unit. The solid black line represents the 1:1 and the dashed lines represent one standard deviation of ± 2 m.

3.4. Contaminant transport model

3.4.1. Transport process

Sulfate transport in groundwater is assumed to follow an advection and dispersion-diffusion process. Furthermore, sulfate is assumed to be non-reactive in groundwater and no retardation occurs. Transport parameters such as effective porosity, molecular diffusion, longitudinal dispersivity and transverse dispersivity that are necessary to consider in each geologic unit are presented in Table 5. As site-specific values are not available, established literature values are used (e.g., McWhorter

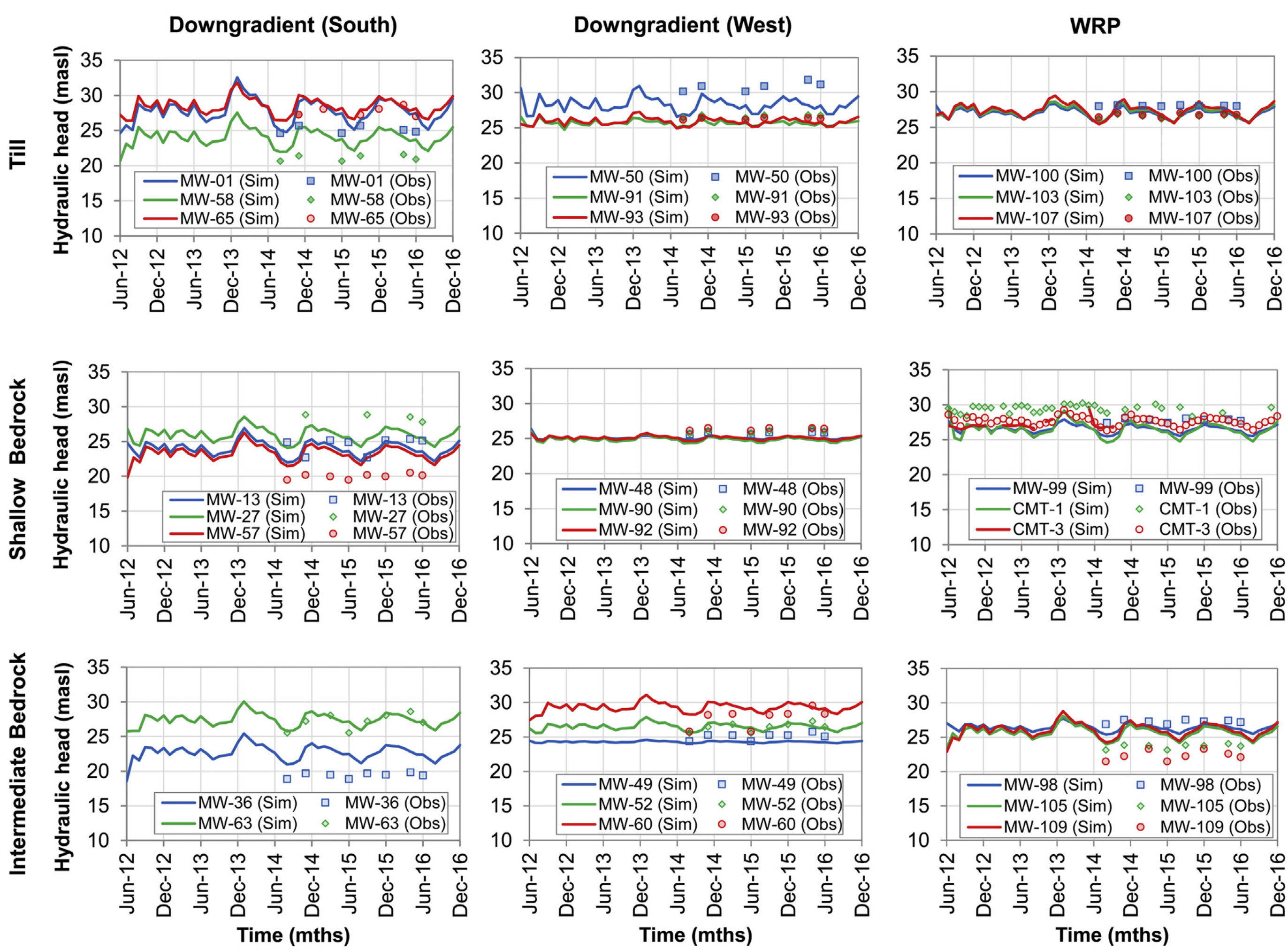

Fig. 5. Distribution of simulated and observed hydraulic heads over time (June 2012 to December 2016) at selected monitoring wells in each geologic unit.

Table 5
Key input parameters to contaminant transport modell.

Parameter	Unit	Overburden	Bedrock
Effective porosity	%	15	5
Molecular diffusion	m^2/s	1×10^{-9}	1×10^{-9}
Longitudinal dispersivity	m	6	3
Transverse dispersivity	m	0.6	0.3

and Sunada, 1977; Domenico and Schwartz, 1990; Schulze-Makuch, 2005).

3.4.2. Long-term source function

The sulfate concentrations measured at the 4 CMT wells between June 2012 and December 2016 are shown in Fig. 7a. Preliminary analysis identified a clear decreasing trend with seasonal variations at all wells, with CMT-2 and CMT-4 displaying the most significant sulfate reductions over time. The location of these wells corresponds to the prominent groundwater flow rates and pathways to the west and northwest (CMT-2) and to the south (CMT-4) of the WRP. Seasonal variations are related to the humid continental climate at the site. For instance, lower concentrations occur during high PPT periods (i.e., spring-melt in April and May and high rainfall in October and November) which causes increased dilution by higher velocity upgradient groundwater. To predict future sulfate concentrations for the long-term source term, the observed monitoring data can be combined with suitable time series analysis.

The multiplicative decomposition method is an analysis method that separates the time series into a trend component that is a smooth function of time, a seasonal component that represents a pattern that is repeated annually, and an error component that is independent for each data point (e.g., Worrall and Burt, 1998; Sizirici and Tansel, 2010; Laner et al., 2012). Sizirici and Tansel (2010) applied the decomposition method to numerous collected leachate quality parameters from a landfill, including total dissolved solids, iron and quantity. The method provided adequate predictions of the future conditions of the parameters and a forecast on the duration of the post-closure period of the closed landfill. In this study, the statistics package Minitab 18 (Minitab 15 StatGuide. Minitab Inc, 2007) was used to apply the time series decomposition method to the observed sulfate concentrations and

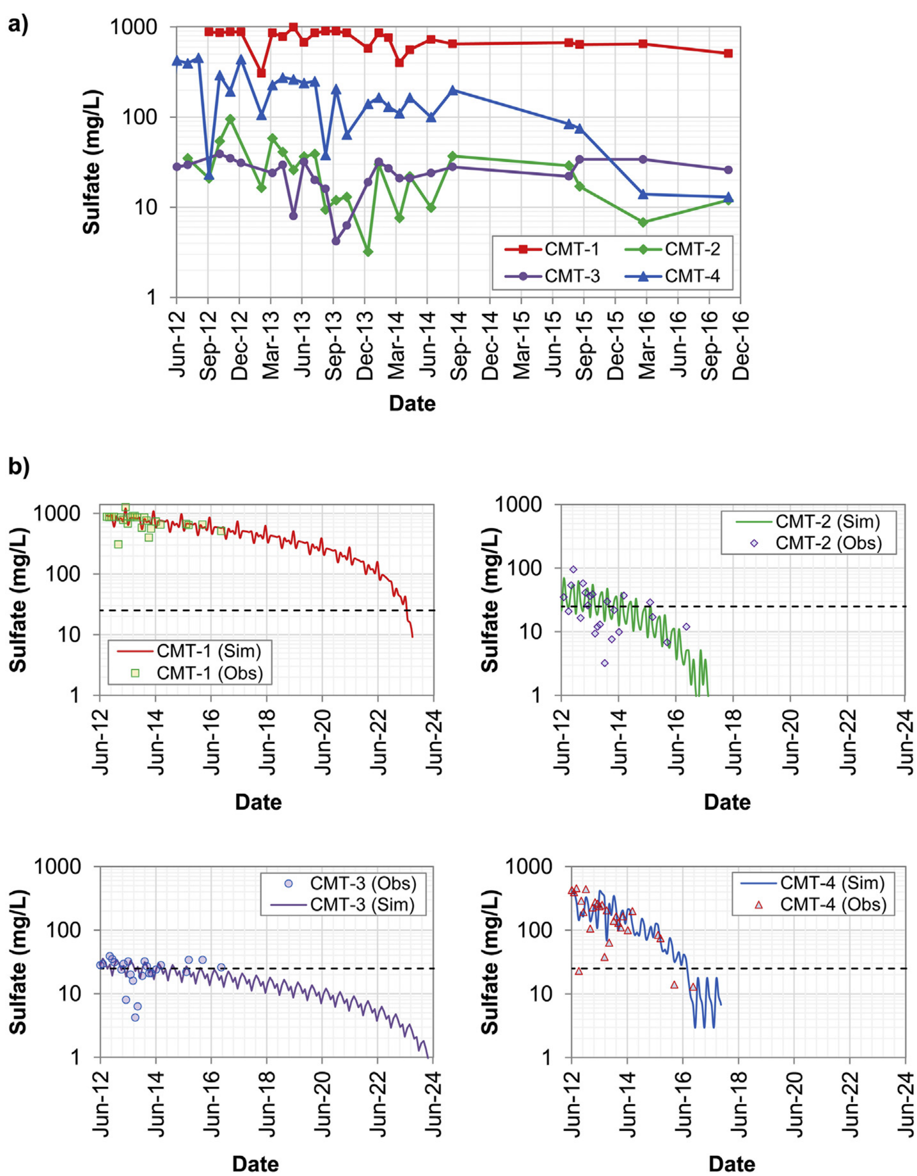

Fig. 7. (a) evolution of sulfate concentrations at each CMT well between June 2012 and November 2016, and (b) time series projections for sulfate concentrations at each CMT well. The black dashed line in (b) represents the background concentration level (BCL) of 25 mg/L.

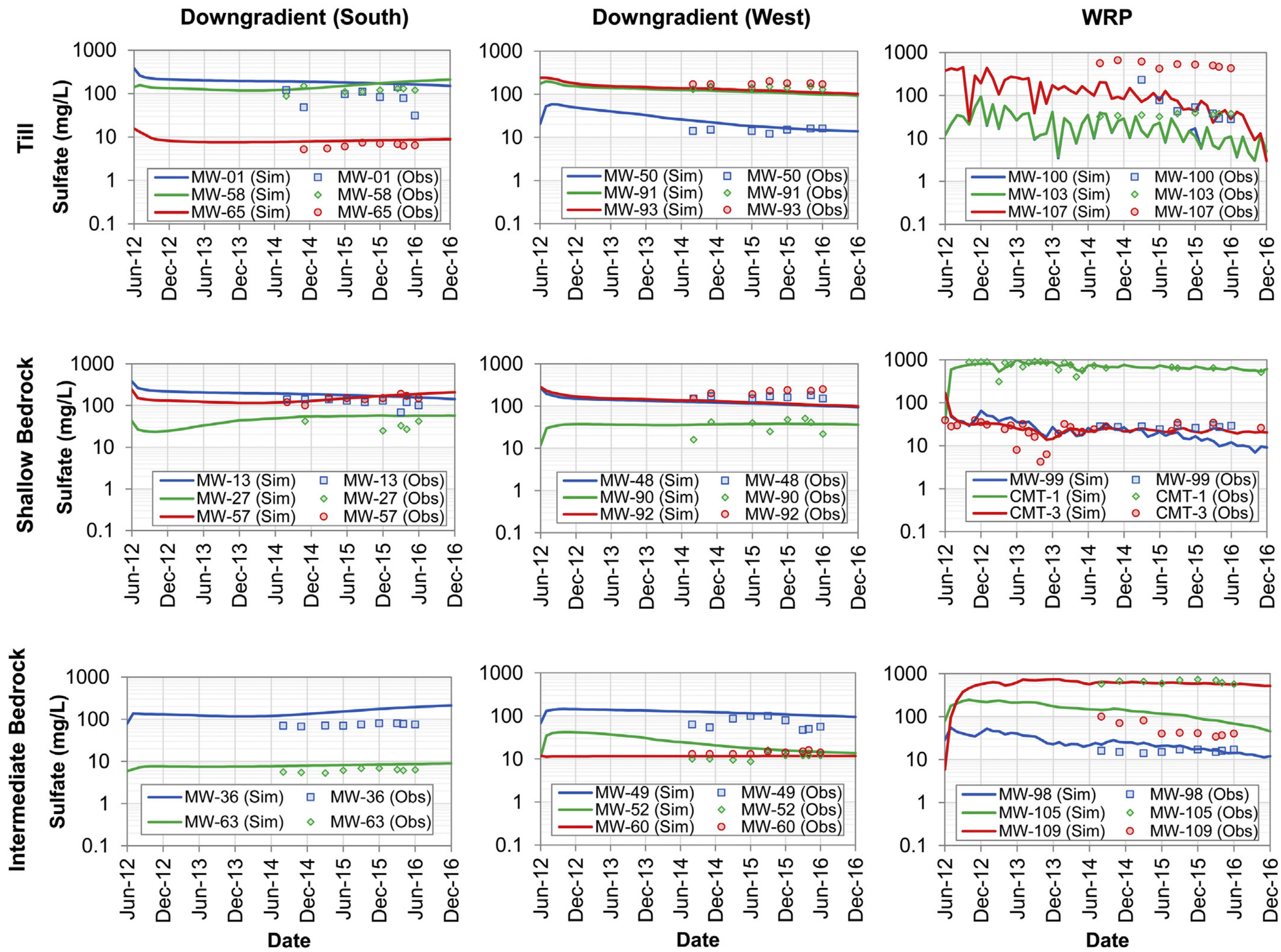

Fig. 8. Distribution of simulated and observed sulfate concentrations with time (June 2012 to December 2016) at selected monitoring wells in each geologic unit.

generate future sulfate source term conditions.

Fig. 7b presents the observed and forecast sulfate concentrations for each CMT well. The background concentration level (BCL) is 25 mg/L which is based on the upgradient groundwater quality measured at the upgradient wells (SCMS-MW-01, −02 and −03). A good fit is evident at all wells between the observed data and forecast data between June 2012 and December 2016. The accuracy of the time series analysis can be expressed by the mean absolute deviation (MAD) and mean absolute percentage error (MAPE), which are expressed in mg/L and %, respectively. The MAD for CMT-1, CMT-2, CMT-3 and CMT-4 are 98.1, 14.1, 7.4 and 71.5, respectively, while the MAPE are 17.9, 71.6, 55.8 and 95.1, respectively. These parameters confirmed the suitability of the selected time series model used and the adequacy of the future sulfate projections (e.g., MAPE values $<$ 80% are considered an adequate fit (e.g., Sizirici and Tansel, 2010)).

From Fig. 7b, it is estimated that sulfate concentrations at CMT-1 will gradually decrease to the BCL by the year 2023. The sulfate concentrations at CMT-2, CMT-3 and CMT-4 decreased to the BCL during the field monitoring period, in 2014, 2014 and 2016, respectively, which was already observed in the field data in Fig. 7a.

The AMD source in the WRP is represented by sulfate concentrations at sparsely distributed point locations. To maintain the spatial and temporal variation in sulfate between all CMT wells, the WRP was divided into separate polygons, with each polygon representing the WRP volume and sulfate source for each CMT well (see Fig. 2). The source distribution over the WRP was estimated from the CMT wells using the Thiessen-polygon method. The sulfate concentrations were assigned to the appropriate polygon within the WRP footprint to the waste rock layers 2, 3 and 4 (Table 1). The predicted sulfate concentrations from Fig. 7b are applied throughout the 50-year simulation period. When the sulfate source at each CMT well reaches the BCL, it attains the BCL value for the remainder of the simulation period.

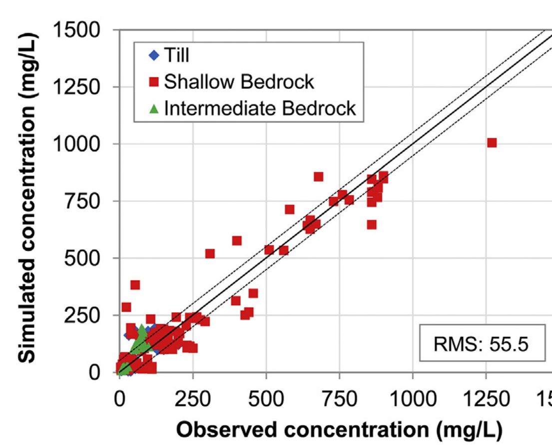

Fig. 9. Transient state comparison of simulated and observed sulfate concentrations in each geologic unit. The solid black line represents the 1:1 and the dashed lines represent one standard deviation of 55.2 mg/L.

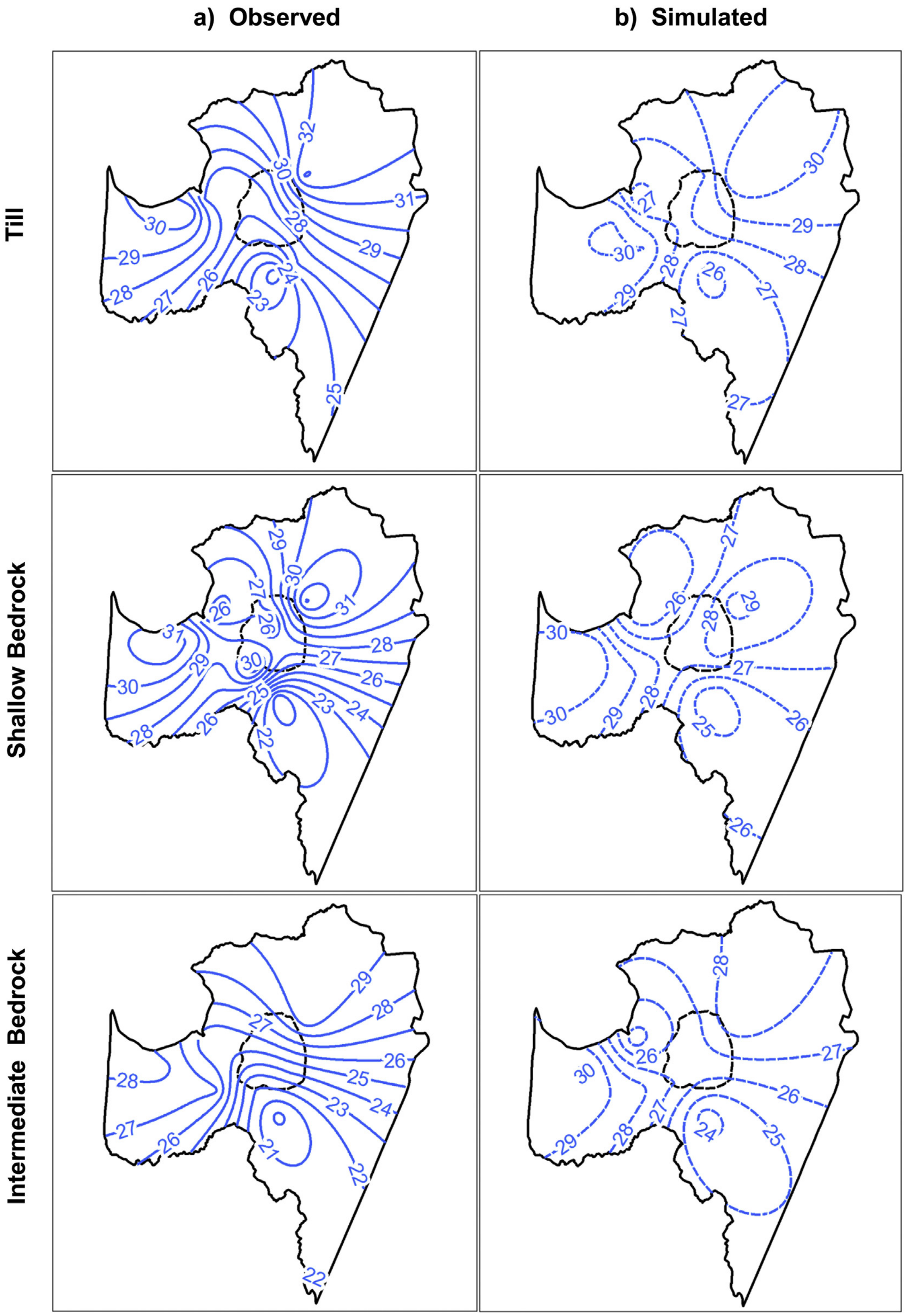

Fig. 10. Comparison of the spatial variations in the 'observed' and 'simulated' hydraulic heads in the till, shallow bedrock and intermediate bedrock units.

3.4.3. Model calibration and verification

The calibrated transient state flow model was used as the basis for the transient transport model. Some trial-and-error calibration was performed as a first step on the observed monitoring data between June 2012 and December 2016. The transport parameters in Table 5 were slightly varied to improve the correlation as much as possible between the observed and simulated sulfate concentrations at all well locations. Fig. 8 presents the simulated and observed sulfate concentrations over time at the same wells presented for the hydraulic heads in Fig. 5. A good correlation exists between observed and simulated sulfate concentrations in each region and geologic unit over the 5-year time period. For instance, seasonal variations in observed sulfate concentrations are repeated in the simulated concentrations at all wells. The CMT wells have the highest sampling density and provide a strong indicator of correlation quality.

The maximum deviations occurred at wells beneath the WRP,

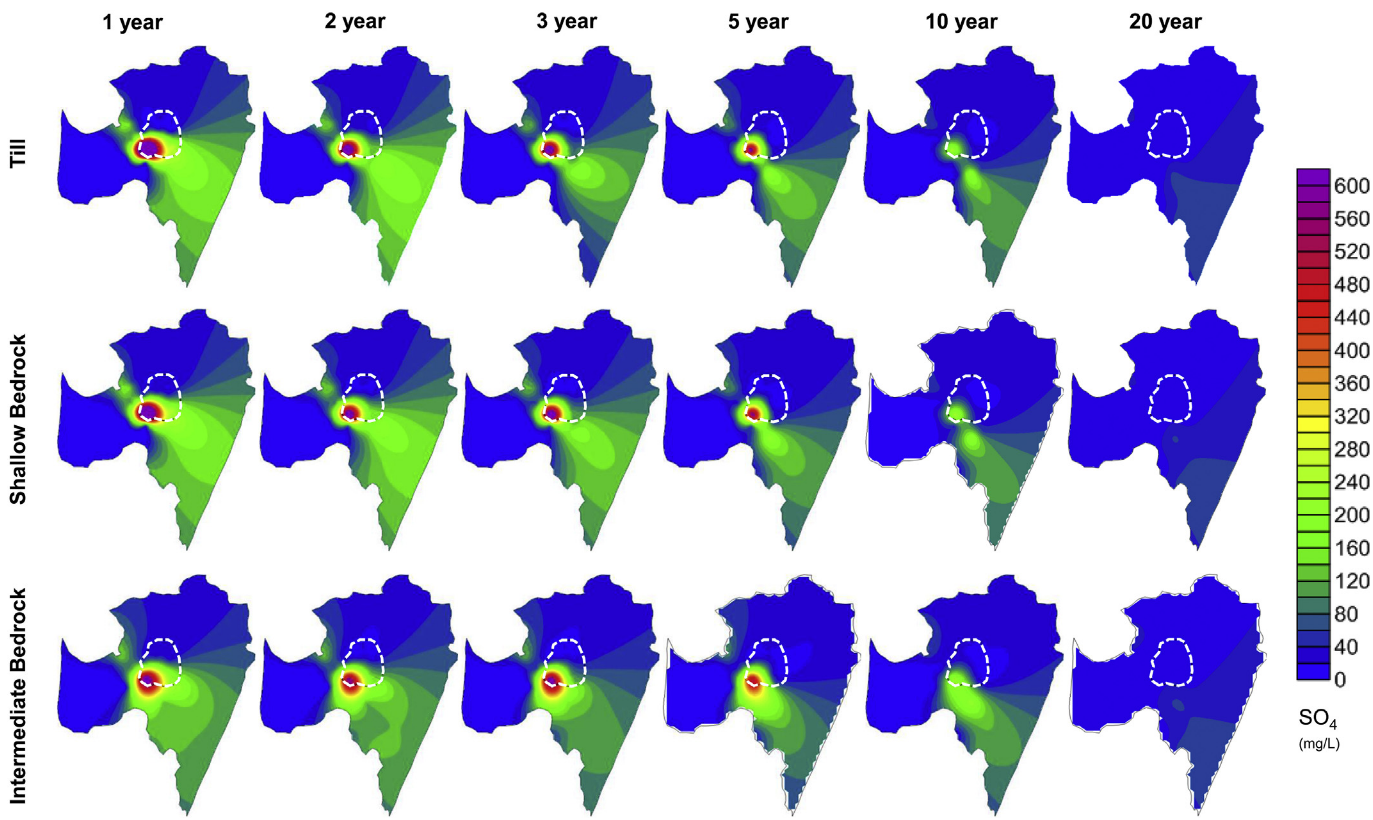

Fig. 11. Spatial distribution of simulated sulfate concentrations in the till, shallow bedrock and intermediate bedrock units.

particularly in the till and intermediate bedrock. This is likely related to the use of the 4 CMT wells in the shallow bedrock to represent the sulfate source in the WRP and therefore may not correlate with sulfate concentrations in the other geological units. The geologic properties of each unit is homogeneous in the model and do not represent the heterogeneity of the sulfate distribution in the observed data. Furthermore, the source for the entire WRP is represented by measured concentrations at 4 sparse locations. Despite these inherent simplifications in the model, a strong correlation generally exists between observed and simulated sulfate concentrations.

Fig. 9 presents a scatter plot diagram of simulated versus observed sulfate concentrations at all CMT and monitoring wells over time. Good agreement is observed at all locations with an RMS error of 2 m. It is evident that the transient flow and transport model has been well calibrated and verified to observed head and sulfate values over the 5-year monitoring period.

The calibrated and verified transient groundwater flow and transport model was then used to simulate the evolution of AMD distribution at the SSSA. The predictive simulations were run for 100 years, using the final conditions established during the calibration and verification process. The long-term simulations provide an indication of remedial performance and/or information on key milestones where concentrations are decreasing below specified guidelines values and/or BCLs.

4. Results and discussion

4.1. Groundwater flow regime

Fig. 10a presents the observed piezometric surface and flow directions in the till, shallow bedrock and intermediate bedrock units in November 2016, which is the last field sampling event available. In all units, groundwater flows from the topographic high to the northeast of the WRP. In the till and shallow bedrock, a groundwater divide exists in an east-west trend through the southern portion of the WRP which generally corresponds with the presence of the low permeability Mullins Coal Seam, and with the surface water divide between the Irish Brook and Kilkenny Lake Brook watersheds. Therefore, groundwater flowing through the WRP is deflected by the groundwater divide, with groundwater in the northern portion flowing in a west to northwestern direction towards Waterford Lake and Irish Brook, while groundwater in the southern portion flows in a south to southeastern direction towards Tributary 1 and Tributary 2. In the intermediate bedrock flow system, all groundwater flows towards the south and southeast.

Fig. 10b also presents the simulated piezometric surface and flow directions in each geological unit. It closely matches the observed groundwater flow regime. Of the 3 units, the best correlations occur in the till and intermediate bedrock. The model generally over-estimates the hydraulic heads south of the WRP. Larger discrepancies occur in the shallow bedrock, with simulated heads higher than observed heads in the southeast, and lower than observed heads in the west (~2 m difference).

4.2. Long-term prediction of AMD distribution

4.2.1. AMD impacts to groundwater

Fig. 11 presents the predicted long-term spatial and temporal distribution of the sulfate contaminant plume at the SSSA. After 1 year, the spatial variation of WRP source concentration is evident within the WRP footprint in each underlying geological unit, with higher concentrations at CMT-1 and CMT-4 compared to CMT-2 and CMT-3. As sulfate seeps from the waste rock into the underlying groundwater, it disperses due to differing flow directions and velocities. As expected, the plume follows the direction of groundwater flow indicated in Fig. 10, with highest downgradient concentrations existing in the west towards Waterford Lake and in the southeast towards Tributary 1 and 2. Although the highest sulfate concentrations occur in the till unit, concentrations are also high in the shallow and intermediate bedrock units due to high vertical hydraulic gradients.

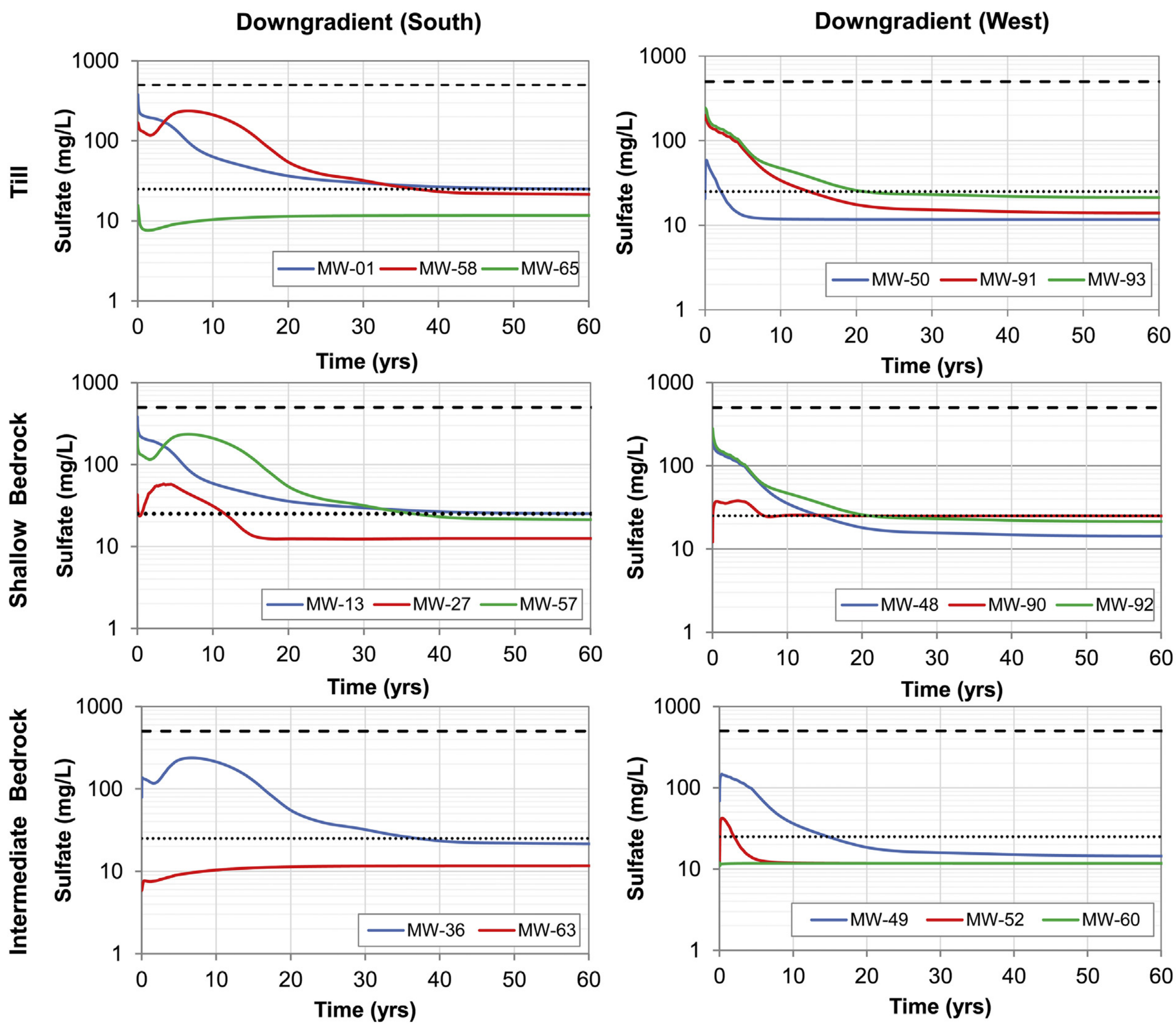

Fig. 12. Prediction of sulfate concentrations at selected monitoring wells in each geologic unit. The black dashed line denotes the Canadian Drinking Water Quality guideline (CDWQ) for sulfate (500 mg/L) and the black dotted line denotes the site background concentration level (BCL) for sulfate (25 mg/L).

Fig. 11 indicates that the sulfate plume concentrations gradually reduces over time, particularly during the first 10 years, thereby highlighting the immediate effectiveness of remediation with an HDPE cover system. At 20 years, the sulfate concentrations have reached, or are approaching, BCLs within all geological units.

To better analyze AMD evolution and cover performance over time, Fig. 12 presents the sulfate concentrations at the same downgradient wells selected for the transient sulfate calibrations in Fig. 8. In addition to the BCL (black dotted line), the Canadian Drinking Water Quality (CDWQ) guideline for sulfate (500 mg/L) is used (black dashed line) to provide a reference for groundwater quality. Fig. 12 confirms that sulfate concentrations at all wells in both downgradient regions were already below the CDWQ guideline at the start of the simulation period. As shown in Fig. 7, CMT-2 and CMT-3 exhibit relatively low sulfate concentrations compared to CMT-1 and CMT-4. As a result, downgradient sulfate concentrations to the west of the WRP, which interact with 'cleaner' groundwater flowing from CMT-2 and CMT-3, decrease more rapidly and reach BCL within 20 years. In contrast, groundwater flowing to the south interacts with CMT-1 and CMT-4, resulting in a slower rate of reduction over time. Nevertheless, all wells to the south reach BCL within 40 years. It is evident from Fig. 12 that the evolution of sulfate concentrations corresponds to the sulfate reduction term shown in Fig. 7.

4.2.2. AMD impacts to surface water

Surface water sampling conducted during the 5-year field monitoring program confirmed significant decreases in sulfate concentrations in all watercourses within the SSSA. The surface water sampling locations indicated in Fig. 2 are associated with the three watercourses related to the key site remedial objectives: SW-01 (Irish Brook), SW-02 (Waterford Lake) and SW-03 (Tributary 2 to Kilkenny Lake Brook). Power et al. (2017) demonstrated that the objectives were already being achieved: (i) water quality in Irish Brook has significantly improved relative to the baseline sulfate concentration of 400 mg/L (sulfate equal to 31 mg/L in November 2016), (ii) water quality in Waterford Lake is protected below the threshold of 17 mg/L (sulfate equal to 5.4 mg/L in November 2016), and (iii) water quality in Tributary 2 is protected within respect to fish habitat threshold of 500 mg/L (sulfate equal to 4.4 mg/L in November 2016).

Significant reductions in AMD impacts to surface water bodies is due to: (i) reductions in AMD loading from covered WRP to groundwater, resulting in improved groundwater quality discharging to surface water, and (ii) elimination of contaminated surface water runoff from previously exposed waste rock that is now overlain with the HDPE-lined cover. Although, detailed modeling of the surface water bodies is outside the scope of this study, long-term stability of the surface water quality with respect to the site remedial objectives can be indirectly obtained by the developed flow and transport model. In

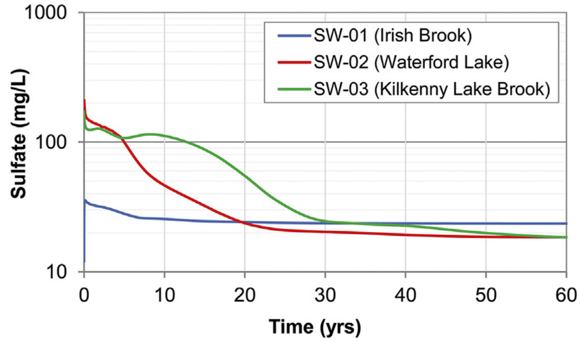

Fig. 13. Long-term sulfate concentrations in groundwater adjacent to key surface water sampling locations.

addition to the monitoring well locations in Fig. 12, the evolution of sulfate concentrations at locations adjacent to SW-01, SW-02 and SW-03 is analyzed. Fig. 13 confirms that groundwater quality improves continuously over time. Therefore, it is evident that surface water quality and site remedial objectives will continue to meet specified performance criteria over the long term.

4.2.3. Sensitivity analysis

A sensitivity analysis was performed to assess key input parameters to the model: NP, aquifer recharge and hydraulic conductivity. An analysis of sulfate concentrations in groundwater adjacent to the key surface water sampling locations is utilized, as shown in Fig. 14.

NP was varied from the base case value of 3% PPT to a minimum of 1% PPT, representative of a near intact cover with limited defects, and a maximum of 34% PPT, representative of conditions with no cover (e.g., King et al., 2003). It is evident from Fig. 14a that decreasing or increasing NP does not affect sulfate concentrations at Irish Brook, which is expected as the sulfate plume does not flow northwards towards Irish Brook. A decrease in NP from 3% PPT to 1% PPT has very little change on sulfate concentrations at Waterford Lake and Kilkenny Lake Brook. Increasing NP to 34% PPT results in a decrease in sulfate concentration at Waterford Lake, which is due to dilution of the low sulfate concentration source seeping from the WRP in this direction (CMT-2 and CMT-3) by the increased seepage water volume, resulting in a lower sulfate loading from the WRP. In contrast, an increase in NP slightly increases the sulfate concentration observed at Kilkenny Lake Brook. The sulfate load seeping from the WRP in this direction (CMT-1 and CMT-4) is much higher due to a combination of high concentration and high seepage rate.

To analyze the sensitivity of the model results to groundwater recharge, the base case recharges (i.e., forested cover = 325 mm; industrial cover = 175 mm; WRP cover = 50 mm) were varied by ± 10%. Fig. 14b presents the variation in groundwater recharge and again shows little to no change in sulfate concentrations near Irish Brook. At Waterford Lake, an increase in recharge results in a significant decrease in sulfate, while a decrease in recharge results in a significant increase in sulfate. This highlights the sensitivity of the sulfate concentration at Waterford Lake to dilution by groundwater recharge, particularly in the forested area between the WRP and Waterford Lake. Similar patterns occurred at Kilkenny Lake Brook, though the changes were much lower due to the increased distance and the observation point at SW-03 not being directly along the flow direction.

Fig. 14c presents the variation in sulfate concentration following changes to hydraulic conductivity at every location and geologic unit by 0.3 orders of magnitude. While sulfate concentrations at Irish Brook show little change, sulfate concentrations at Waterford Lake and Kilkenny Lake Brook exhibit more significant changes. An increase in hydraulic conductivity results in an increase in groundwater flow velocity and dilution and a corresponding decrease in sulfate concentration. Similarly, a decrease in hydraulic conductivity results in a decrease in groundwater dilution and increased sulfate concentrations. The magnitude of these changes in sulfate concentration are more significant at Kilkenny Lake Brook due to the increased distance and flow volume from the WRP.

4.3. Landform stability and vegetation

Although the WRP has relatively low slopes, some erosion was visible at sparse locations. This is due to the absence of a drainage layer above the HDPE, with the associated high pore-water pressures and saturation and the loss in shear strength in the soil layer resulting in localized surface ponding and discharge areas. Vegetation surveys indicated that the vegetative composition is thriving, with soil profiles showing that root depths do not exceed 20 cm and thereby do not provide a risk to HDPE liner integrity.

4.4. Limitations

A number of simplifying assumptions were used in this numerical study. It is acknowledged that WRPs and geologic units can be complex and heterogeneous and the assumption of homogeneity at the presented study site is simplistic. This assumption simplifies water flow and contaminant distribution in the WRP and receiving environment. Hydraulic conductivity is a critical parameter in groundwater flow and contaminant transport and poorly representative values can lead to significant underestimation or overestimation of hydraulic heads, as evident during calibration of the study site model. Furthermore, associated discrepancies in groundwater flow velocities can lead to inaccuracies in contaminant concentrations which is particularly important for long-term predictions. Nevertheless, it is common in large and complex study areas to assume representative mean values. An extensive geological database was available for the study site and a narrow range of conductivity values existed. The mean values used were carefully selected and subsequently adjusted during the model development to obtain a well-calibrated and verified groundwater flow and contaminant transport model.

Knowledge on the quality of AMD water seeping from the base of the WRP is essential to accurately assess and predict AMD release/depletion rates within the WRP and loading to the receiving environment. At the study site, waste rock pore-water samples could not be obtained so groundwater samples from the underlying shallow bedrock were used. As a result, AMD loading is likely underestimated as it based on groundwater concentrations that may have already diminished due to dilution with upgradient groundwater. To more accurately access the annual generation and release of AMD to groundwater, various kinetic and reactive aspects can be incorporated. Current work involves laboratory experiments with humidity cells and leaching columns on waste rock samples extracted from the WRP to assess various kinetic aspects such as the velocity of sulfide oxidation and metal leaching rates.

The contaminant transport component simulated advective and dispersive-diffusive transport of sulfate in groundwater. It was assumed that the sulfate was non-reactive and no retardation occurs. Future work will couple the PHREEQC geochemical reaction model (Charlton and Parkhurst, 2011) with the FEFLOW model to include kinetic and multiphase transfer processes for improved predictions of long-term AMD generation, release and transport from the WRP.

A challenging component of long-term predictive modeling studies is incorporating future variations in climate which significantly impact key parameters such as groundwater recharge (including NP) and acidity loading. At the study site, PPT and recharge were measured over a 5-year monitoring period and used to estimate monthly recharge as a percentage of PPT. A 30-year climatic database (1981 to 2010) was then used to provide long-term PPT that accounts for climatic variations and corresponding long-term recharge using the monthly percentage of PPT. Additionally, long-term sulfate concentrations seeping from the

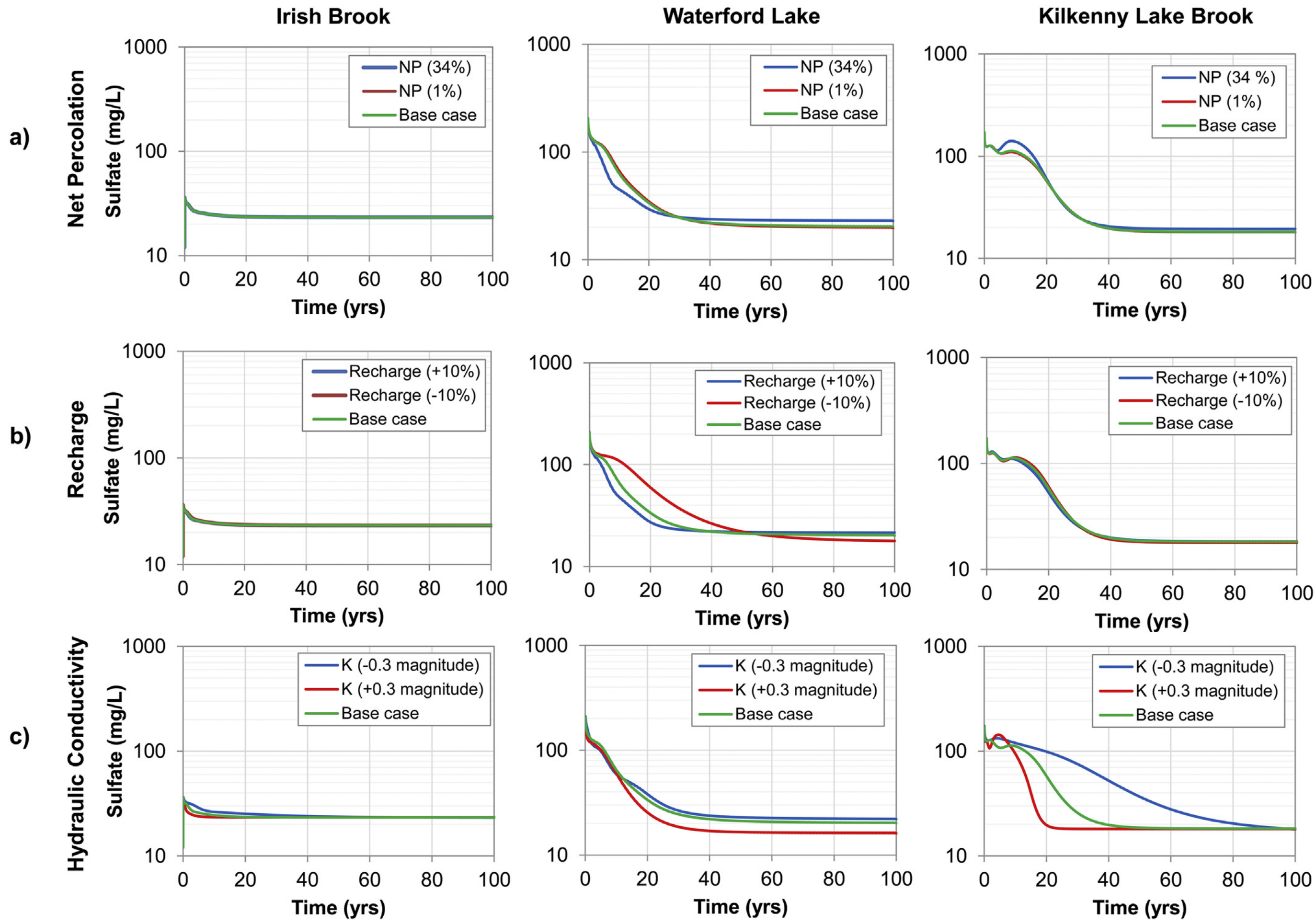

Fig. 14. Sensitivity analysis on sulfate concentrations in groundwater adjacent to key surface water sampling locations.

WRP were estimated from time-series analysis of the sulfate concentrations measured during the 5-year monitoring period. Soil-atmosphere and seepage models calibrated to measured field data may improve future predictions of recharge and seepage rates in covered WRPs.

While this study has demonstrated that HDPE-lined cover systems can be highly effective for reducing long-term AMD impacts to the receiving environment, the integrity and service life of the geomembrane need to be considered. Oxidative degradation of the HDPE over time will decrease properties such as strength and stress crack resistance (Rowe, 2012). It should be noted that different HDPE liners will have different antioxidant packages and depletion times, which directly influence service life. For instance, HDPE thickness has a significant effect on antioxidant depletion, with 2.5 mm thick HDPE taking approximately 50% longer to deplete than 1.5 mm thick HDPE (Rowe et al., 2010). Service temperature has a significant effect on HDPE performance, with higher temperatures resulting in shorter service life (Rowe and Ewais, 2015). While the WRP in this study lies within a humid continental climate with temperatures typically < 30 °C, WRPs in other climates such as semi-arid or arid will experience much higher temperatures and shorter HDPE service life. A detailed discussion on the service life of HDPE is provided by Rowe (2012).

5. Conclusions

In this study, a numerical investigation was performed to investigate the long-term effectiveness of HDPE-lined cover systems installed over acid-generating WRPs. A remediated former mining site in Nova Scotia, Canada contains a WRP that was overlain with an HDPE cover in 2011. A 3-D groundwater flow and contaminant transport model of the study site, including the WRP and environmental receptors, was developed in FEFLOW. Key hydrogeological and geochemical field data collected during extensive post-remediation field monitoring between January 2012 and December 2016 were used to effectively calibrate and verify the model. The cover system generated a ~90% reduction in water flux into the WRP (i.e., 512 to 50 mm/year), resulting in reduced AMD generation and seepage from the WRP into groundwater.

The model was used to simulate the long-term spatial and temporal evolution of AMD over 100 years. Results indicated continual improvements in groundwater quality over time with groundwater quality reaching background water quality (i.e., < 25 mg/L) within 40 years. Although the model confirmed groundwater quality will improve over time, key site remedial objectives were related to surface water quality. Since the 5-year field monitoring program confirmed that each remedial objective related to surface water quality was already being achieved, the groundwater model was used to confirm that groundwater quality adjacent to the relevant surface water bodies will be maintained and/or continue to improve over the long-term. Therefore, although surface water modeling was beyond the scope of this study, the groundwater model was able to indirectly indicate that key remedial objectives will be achieved.

This study has demonstrated the long-term effectiveness of remedial activities involving HDPE-lined cover systems to significantly reduce the impacts of AMD on a WRP receiving environment. While the study focused on one field site, the approach and findings are applicable to other WRP sites. Furthermore, it should be noted that the performance of the cover system will evolve over time in response to climatic conditions and site-specific physical, chemical and biological processes that are extremely difficult to predict. Periodic in situ monitoring and physical studies of processes such as freeze-thaw, vegetation and erosion cycles are recommended to maintain a rigorous evaluation of long-term remedial performance.

Acknowledgements

This work was conducted under the CAPs Monitoring Project and funded by Enterprise Cape Breton Corporation (ECBC) which was later dissolved into Public Works and Government Services Canada (PWGSC). The authors would like to give special thanks to Joseph MacPhee and Joseph Shea (PWGSC) and Devin MacAskill (Cape Breton Regional Municipality, CBRM) for their support during this study. The authors wish to thank O'Kane Consultants for technical advice during this study, along with David Mayich and Fred Baechler (exp Consultants). Thanks are also given to Jamie Tunnicliff (Stantec Consulting Ltd.) for providing the post-remediation groundwater monitoring well data.

References

Adu-Wusu, C., Yanful, E.K., 2006. Performance of engineered test covers on acid-generating waste rock at Whistle mine, Ontario. Can. Geotech. J. 43 (1), 1–18. https://doi.org/10.1139/t05-088.

Agbenyeku, E.E., Muzenda, E., Msibi, M.I., 2017. Provisional equations for determining leachate leakage rate through composite barriers from compromised geomembrane. Proc. Manufact. 7, 277–283. https://doi.org/10.1016/j.promfg.2016.12.070.

Albrecht, B.A., Benson, C.H., 2001. Effect of desiccation on compacted natural clays. J. Geotech. Geoenviron. Eng. 127 (1), 67–75. https://doi.org/10.1061/(ASCE)1090-0241(2001)127:1(67).

Amos, R.T., Blowes, D.W., Bailey, B.L., Sego, D.C., Smith, L., Ritchie, A.I.M., 2015. Waste-rock hydrogeology and geochemistry. Appl. Geochem. 57, 140–156. https://doi.org/10.1016/j.apgeochem.2014.06.020.

Anderson, M.P., Woessner, W.W., Hunt, R.J., 2015. Applied Groundwater Modeling: Simulation of Flow and Advective Transport. Academic Press ISBN 0080916384.

Ayres, B., Dirom, G., Christensen, D., Januszewski, S., O'Kane, M., 2003. Performance of cover system field trials for waste rock at Myra Falls Operations. In: Farrell, T., Taylor, G. (Eds.), Proceedings of the 6th International Conference on Acid Rock Drainage (ICARD). 1875776982, (12–18 July, Cairns.).

Benson, C., 2000. Liners and covers for waste containment. In: Proceedings of the Fourth Kansai International Geotechnical Forum, Creation of a New Geo-Environment. Japanese Geotechnical Society, Kyoto, Japan, pp. 1–40.

Benson, C.H., Daniel, D.E., Boutwell, G.P., 1999. Field performance of compacted clay liners. J. Geotech. Geoenviron. Eng. 125 (5), 390–403. https://doi.org/10.1061/(ASCE)1090-0241(1999)125:5(390).

Benson, C.H., Thorstad, P.A., Jo, H.Y., Rock, S.A., 2007. Hydraulic performance of geosynthetic clay liners in a landfill final cover. J. Geotech. Geoenviron. 133 (7), 814–827. https://doi.org/10.1061/(ASCE)1090-0241(2007)133:7(814).

Blowes, D.W., 1997. The environmental effects of mine wastes. In: Gubins, A.G. (Ed.), Proceedings of Exploration 97. Fourth Decennial International Conference on Mineral Exploration, Toronto, pp. 887–892.

Bordeleau, G., Martel, R., Schäfer, D., Ampleman, G., Thiboutot, S., 2008. Groundwater flow and contaminant transport modelling at an air weapons range. Environ. Geol. 55, 385. https://doi.org/10.1007/s00254-007-0984-3.

Cartaud, F., Goblet, P., Touze-Foltz, N., 2005. Numerical simulation of the flow in the interface of a composite bottom liner. Geotext. Geomembr. 23 (6), 513–533. https://doi.org/10.1016/j.geotexmem.2005.04.002.

Cazaux, D., Didier, G., 2000. Field evaluation of hydraulic performances of geosynthetic clay liners by small and large-scale tests. Geotext. Geomembr. 18 (2), 163–178. https://doi.org/10.1016/S0266-1144(99)00025-4.

Chappel, M.J., Brachman, R.W.I., Take, W.A., Rowe, R.K., 2012. Large-scale quantification of wrinkles in a smooth black HDPE geomembrane. J. Geotech. Geoenviron. 138 (6), 671–679. https://doi.org/10.1061/(ASCE)GT.1943-5606.0000643.

Charlton, S.R., Parkhurst, D.L., 2011. Modules based on the geochemical model PHREEQC for use in scripting and programming languages. Comput. Geosci. 37 (10), 1653–1663. https://doi.org/10.1016/j.cageo.2011.02.005.

Chopra, M., Rastogi, R., Kumar, A.V., Sunny, F., Nair, R.N., 2013. Response surface method coupled with first-order reliability method based methodology for groundwater flow and contaminant transport model for the uranium tailings pond site. Environ. Model. Assess. (2013), 18. 439. https://doi.org/10.1007/s10666-012-9352-0.

Colucci, P., Lavagnolo, M.C., 1995. Three years field experience in electrical control of synthetic landfill liners. In: Christensen, T.H., Cossu, R., Stegmann, R. (Eds.), Proceedings of the 5th International Landfill Symposium, Santa Margherita di Pula, Cagliari, Italy, 2–6 October 1995. CISA, Environmental Sanitary Engineering Centre, Cagliari, Italy, pp. 437–452.

Diersch, H.J.G., 2014. FEFLOW: Finite element modeling of flow, mass and heat transport in porous and fractured media. Springer-Verlag, Berlin, pp. 996. https://doi.org/10.1007/978-3-642-38739-5.

Domenico, P.A., Schwartz, F.W., 1990. Physical and Chemical Hydrogeology — Hydraulic Testing: Models, Methods, and Applications. John Wiley & Sons Inc., New York (reprinted by permission of John Wiley & Sons Ltd.) (1990).

Elango, L., Brindha, K., Kalpana, L., Sunny, F., Nair, R.N., Murugan, R., 2012. Groundwater flow and radionuclide decay-chain transport modelling around a proposed uranium tailings pond in India. Hydrogeol. J. 20, 797. https://doi.org/10.1007/s10040-012-0834-6.

Environment Canada, 2017. Historical Weather Data. http://climate.weather.gc.ca/historical_data/search_historic_data_e.html Accessed 25 Aug 2017.

Fala, O., Molson, J., Aubertin, M., Bussière, B., 2005. Numerical modelling of flow and capillary barrier effects in unsaturated waste rock piles. Mine Water Environ. 24 (4), 172–185. https://doi.org/10.1007/s10230-005-0093-z.

Fala, O., Molson, J., Aubertin, M., Dawood, I., Bussière, B., Chapuis, R.P., 2013. A numerical modelling approach to assess long-term unsaturated flow and geochemical transport in a waste rock pile. Int. J. Min. Reclam. Environ. 27 (1), 38–55. https://doi.org/10.1080/17480930.2011.644473.

Giroud, J.P., Badu-Tweneboah, K., Bonaparte, R., 1992. Rate of leakage through a composite liner due to geomembrane defects. Geotext. Geomembr. 11 (1), 1–28. https://doi.org/10.1016/0266-1144(92)90010-8.

Hopp, L., McDonnell, J.J., Condon, P., 2011. Lateral subsurface flow in a soil cover over waste rock in a humid temperate environment. Vadose Zone J. 10 (1), 332–344. https://doi.org/10.2136/vzj2010.0094.

INAP (The International Network for Acid Prevention), 2014. Global acid rock drainage guide. http://gardguidecom/images/5/5f/TheGlobalAcidRockDrainageGuide.pdf Accessed 14 April 2017.

Kefeni, K.K., Msagati, T.A., Mamba, B.B., 2017. Acid mine drainage: prevention, treatment options, and resource recovery: a review. J. Clean. Prod. 151, 475–493. https://doi.org/10.1016/j.jclepro.2017.03.082.

Kim, H., Benson, C.H., 2004. Contributions of advective and diffusive oxygen transport through multilayer composite caps over mine waste. J. Contam. Hydrol. 71, 193–218. https://doi.org/10.1016/j.jconhyd.2003.10.001.

King, M., Check, G., Carey, G., Abbey, D., Baechler, F., 2003. Groundwater and contaminant transport modelling at the Sydney Tar Ponds. In: Canadian Geotechnical Society. Proceedings of 56th Annual Canadian Geotechnical Conference and 4th Joint IAH-CNC/CGS Groundwater Specialty Conference, September 29–October 1, 2003, Winnipeg.

Koerner, R.M., Hsuan, Y.G., Koerner, G.R., 2011. Geomembrane lifetime prediction: unexposed and exposed conditions. In: GRI White Paper No. 6. Geosynthetic Institute (Updated February 2011, 27 pp.).

Laner, D., Crest, M., Scharff, H., Morris, J.W., Barlaz, M.A., 2012. A review of approaches for the long-term management of municipal solid waste landfills. Waste Manag. 32 (3), 498–512. https://doi.org/10.1016/j.wasman.2011.11.010.

Lefebvre, R., Hockley, D., Smolensky, J., Lamontagne, A., 2001. Multiphase transfer processes in waste rock piles producing acid mine drainage: 2. Applications of numerical simulation. J. Contam. Hydrol. 52 (1), 165–186. https://doi.org/10.1016/S0169-7722(01)00157-7.

Li, Y., Li, J.L., Chen, S., Diao, W., 2012. Establishing indices for groundwater contamination risk assessment in the vicinity of hazardous waste landfills in China. Environ. Pollut. 165, 77–90. https://doi.org/10.1016/j.envpol.2011.12.042.

Lupo, J.F., Morrison, K.F., 2007. Geosynthetic design and construction approaches in the mining industry. Geotext. Geomembr. 25 (2), 96–108. https://doi.org/10.1016/j.geotexmem.2006.07.003.

McWhorter, D.B., Sunada, D.K., 1977. Ground-water hydrology and hydraulics. In: Water Resources Publication, ISBN 0918334187, 9780918334183.

Meer, S.R., Benson, C.H., 2007. Hydraulic conductivity of geosynthetic clay liners exhumed from landfill final covers. J. Geotech. Geoenviron. Eng. 133 (5), 550–563. https://doi.org/10.1061/(ASCE)1090-0241(2007)133:5(550).

Meiers, G., Bradley, C., 2017. The critical role of lateral drainage capacity in limiting leakage through a low permeability geomembrane cover. In: Proceedings of Geotechnical Frontiers 2017, 12–15 March 2017. ASCE. https://doi.org/10.1061/9780784480434.013.

Meiers, G., O'Kane, M., Barbour, S.L., 2009. Measuring net percolation rates for waste storage facility cover systems. In: Canadian Geotehnical Society. Proceedings of 62nd Canadian Geotechnical Conference, 20–24 September 2009, Halifax, Nova Scotia, Canada, ISBN 0920505198.

Meiers, G., O'Kane, M., Mayich, D., 2011. Evaluating the performance of a high density polyethylene lined cover system at the reclaimed Franklin Mine near Sydney, Canada. In: Fourie, A.B., Tibbett, M., Beersing, A. (Eds.), Mine Closure 2011: Proceedings of the Sixth International Conference on Mine Closure, 18–21 September 2011, Alberta, Canada. Australian Centre for Geomechanics, Perth ISBN 9780987093714.

MEND (Mine Environment Neutral Drainage), 2004. Design, construction and performance monitoring of cover systems for waste rock and tailings: volume 1—summary. In: Canadian Mine Environment Neutral Drainage Program, Project 2.21.4a, July 2004, . http://mend-nedem.org/wp-content/uploads/2.21.4a-Cover-Design-Manual.pdf Accessed 15 February 2017.

MEND (Mine Environment Neutral Drainage), 2012. Cold regions cover system design technical guidance document. In: Canadian Mine Environment Neutral Drainage Program, Project 1.61.5c, in progress. http://mend-nedem.org/wp-content/uploads/2013/01/1.61.5c.pdf Accessed 20 August 2017.

Minitab 15 StatGuide. Minitab Inc, 2007. Minitab Statistical Software, Release 15 for Windows. State College, Pennsylvania.

Molson, J.W., Fala, O., Aubertin, M., Bussière, B., 2005. Numerical simulations of pyrite oxidation and acid mine drainage in unsaturated waste rock piles. J. Contam. Hydrol. 78 (4), 343–371. https://doi.org/10.1016/j.jconhyd.2005.06.005.

Needham, A.D., Gallagher, E.M.G., Smith, J.W.N., 2004. Prediction of the long term generation of defects in HDPE liners. In: Proceedings of the Third European Conference on Geosynthetics, Munich, Germany, pp. 2 507e514.
Needham, A.D., Smith, J.W.N., Gallagher, E.M.G., 2006. The service life of polyethylene geomembrane barriers. Eng. Geol. 85 (1e2), 82e90.
Nordstrom, D.K., Blowes, D.W., Ptacek, C.J., 2015. Hydrogeochemistry and microbiology or mine drainage: an update. Appl. Geochem. 57, 3–16. https://doi.org/10.1016/j.apgeochem.2015.02.008.
Nosko, V., Touze-Foltz, N., 2000. Geomembrane liner failure: modeling of its influence on contaminant transfer. In: Proceedings of the 2nd European Geosynthetics Conference, Bologna, Italy, 15–18 October 2000, pp. 557–560.
O'Kane, M., Ayres, B., 2012. Cover systems that utilise the moisture store-and-release concept–do they work and how can we improve their design and performance? In: Fourie, A.B., Tibbett, M. (Eds.), Proc 7th International Conf on Mine Closure. Australian Centre for Geomechanics, pp. 407–415.
Orban, P., Brouyère, S., Batlle-Aguilar, J., Couturier, J., Goderniaux, P., Leroy, M., Maloszewski, P., Dassargues, A., 2010. Regional transport modelling for nitrate trend assessment and forecasting in a chalk aquifer. J. Contam. Hydrol. 118 (1), 79–93. https://doi.org/10.1016/j.jconhyd.2010.08.008.
Othman, M.A., Benson, C.H., 1993. Effect of freeze–thaw on the hydraulic conductivity and morphology of compacted clay. Can. Geotech. J. 30 (2), 236–246. https://doi.org/10.1139/t93-020.
Power, C., Gerhard, J.I., Karaoulis, M., Tsourlos, P., Giannopoulos, A., 2014. Evaluating four-dimensional time-lapse electrical resistivity tomography for monitoring DNAPL source zone remediation. J. Contam. Hydrol. 162–163, 27–46. https://doi.org/10.1016/j.jconhyd.2014.04.004.
Power, C., Ramasamy, M., MacAskill, D., Shea, J., MacPhee, J., Mayich, D., Baechler, F., Mkandawire, M., 2017. Five-year performance monitoring of a high-density polyethylene (HDPE) cover system at a reclaimed mine waste rock pile in the Sydney Coalfield (Nova Scotia, Canada). Environ. Sci. Pollut. Res. 24 (34), 26744–26762. https://doi.org/10.1007/s11356-017-0288-4.
Power, C., Ramasamy, M., Mkandawire, M., 2018a. Performance assessment of a single-layer moisture store-and-release cover system at a mine waste rock pile in a seasonally humid region (Nova Scotia, Canada). Environ. Monit. Assess. 190, 186. https://doi.org/10.1007/s10661-018-6555-0.
Power, C., Tsourlos, P., Ramasamy, M., Nivorlis, A., Mkandawire, M., 2018b. Combined DC resistivity and induced polarization (DC-IP) for mapping the internal composition of a mine waste rock pile in Nova Scotia, Canada. J. Appl. Geophys. Online. 150, 40–51. https://doi.org/10.1016/j.jappgeo.2018.01.009.
PWGSC (Public Works and Government Services Canada), 2013. Enterprise Cape Breton Corporation Former Mine Site Closure Program: Update 2013–2014. http://www.ecbc-secb.gc.ca/upload/ECBC_SiteClosure2013_English1387296888.pdf Accessed 20 Apr 2017.
Rollin, A.L., Marcotte, M., Chaput, L., 2002. Lessons learned from geoelectrical leaks surveys. In: Proceedings of the Seventh International Conference on Geosynthetics, Nice, France, pp. 2 527e530.
Rowe, R.K., 2005. Long-term performance of contaminant barrier systems. Geotechnique 55 (9), 631–678.
Rowe, R.K., 2012. Short- and long-term leakage through composite liners. The 7th Arthur Casagrande Lecture. Can. Geotech. J. 49 (2), 141–169. https://doi.org/10.1139/t11-092.
Rowe, R.K., Ewais, A.M.R., 2015. Ageing of exposed geomembranes at locations with different climatological conditions. Can. Geotech. J. 52 (3), 326–343. https://doi.org/10.1139/cgj-2014-0131.
Rowe, R.K., Rimal, S., Sangam, H., 2009. Ageing of HDPE geomembranes exposed to air, water and leachate at different temperatures. Geotext. Geomembr. 27 (2), 137–151. https://doi.org/10.1016/j.geotexmem.2008.09.007.
Rowe, R.K., Islam, M.Z., Hsuan, Y.G., 2010. Effect of thickness on the ageing of HDPE geomembranes. J. Geotech. Geoenviron. 136 (2), 299–309. https://doi.org/10.1061/(ASCE)GT.1943-5606.0000207.
Rowe, R.K., Chappel, M.J., Brachman, R.W.I., Take, W.A., 2012. Field study of wrinkles in a geomembrane at a composite liner test site. Can. Geotech. J. 49 (10), 1196–1211. https://doi.org/10.1139/t2012-083.
Sangam, H.P., Rowe, R.K., 2002. Effects of exposure conditions on the depletion of antioxidants from HDPE geomembranes. Can. Geotech. J. 39, 1221–1230. https://doi.org/10.1139/t02-074.
Scanlon, B.R., Reedy, R.C., Keese, K.E., Dwyer, S.F., 2005. Evaluation of evapotranspirative covers for waste containment in arid and semiarid regions in the southwestern USA. Vadose Zone J. 4 (1), 55–71. https://doi.org/10.2113/4.1.55.
Schulze-Makuch, D., 2005. Longitudinal dispersivity data and implications for scaling behavior. Ground Water 43, 443–456. https://doi.org/10.1111/j.1745-6584.2005.0051.x.
Şengör, S.S., Ünlü, K., 2013. Modeling contaminant transport and remediation at an acrylonitrile spill site in Turkey. J. Contam. Hydrol. 150, 77–92. https://doi.org/10.1016/j.jconhyd.2013.02.010.
Simate, G.S., Ndlovu, S., 2014. Acid mine drainage: challenges and opportunities. J. Environ. Chem. Eng. 2 (3), 1785–1803. https://doi.org/10.1016/j.jece.2014.07.021.
Sizirici, B., Tansel, B., 2010. Projection of landfill stabilization period by time series analysis of leachate quality and transformation trends of VOCs. Waste Manag. 30 (1), 82–91. https://doi.org/10.1016/j.wasman.2009.09.006.
Song, Q., Yanful, E.K., 2008. Monitoring and modeling of sand-bentonite cover for ARD mitigation. Water Air Soil Pollut. 190, 65. https://doi.org/10.1007/s11270-007-9581-z.
Take, W.A., Chappel, M.J., Brachman, R.W.I., Rowe, R.K., 2007. Quantifying geomembrane wrinkles using aerial photography and digital image processing. Geosynth. Int. 14 (4), 219–227. https://doi.org/10.1680/gein.2007.14.4.219.
Thiel, R., Smith, M.E., 2004. State of the practice review of heap leach pad design issues. Geotext. Geomembr. 22, 555–568. https://doi.org/10.1016/j.geotexmem.2004.05.002.
Touze-Foltz, N., Giroud, J.P., 2003. Empirical equations for calculating the rate of liquid flow through composite liners due to geomembrane defects. Geosynth. Int. 10 (6), 215e233.
Worrall, F., Burt, T.P., 1998. Decomposition of river water nitrate time-series—comparing agricultural and urban signals. Sci. Total Environ. 210/211, 153–162. https://doi.org/10.1016/S0048-9697(98)00048-5.
Yanful, E.K., 1993. Oxygen diffusion through soil covers on sulphidic mine tailings. J. Geotech. Eng. 119 (8), 1207–1228. https://doi.org/10.1061/(ASCE)0733-9410(1993)119:8(1207).
Yanful, E.K., Simms, P.H., Rowe, R.K., Stratford, G., 1999. Monitoring an experimental soil waste near London, Ontario, Canada. Geotech. Geol. Eng. 17 (2), 65–84. https://doi.org/10.1023/A:1008986103460.